International Journal of Machine Consciousness
Vol. 4, No. 1 (2012) 109−140

DOI: 10.1142/S1793843012400069

World Scientific
www.worldscientific.com

NON-DESTRUCTIVE WHOLE-BRAIN MONITORING USING NANOROBOTS: NEURAL ELECTRICAL DATA RATE REQUIREMENTS

NUNO R. B. MARTINS* and WOLFRAM ERLHAGEN†

Center for Mathematics,
University of Minho, Campos de Azurem,
Guimarães 4800-058, Portugal
**n-martins@n-martins.com*
†*wolfram.erlhagen@math.uminho.pt*

ROBERT A. FREITAS JR.

Institute for Molecular Manufacturing,
555 Bryant Street, Suite 354,
Palo Alto, California 94301, USA
rfreitas@rfreitas.com

Neuronanorobotics, a promising future medical technology, may provide the ultimate tool for achieving comprehensive non-destructive real-time *in vivo* monitoring of the many information channels in the human brain. This paper focuses on the electrical information channel and employs a novel electrophysiological approach to estimate the data rate requirements, calculated to be $(5.52 \pm 1.13) \times 10^{16}$ bits/sec in an entire living human brain, for acquiring, transmitting, and storing single-neuron electrical information using medical nanorobots, corresponding to an estimated synaptic-processed spike rate of $(4.31 \pm 0.86) \times 10^{15}$ spikes/sec.

Keywords: Human brain information; medical nanorobotics; nanomedicine; nanorobot; nanotechnology; neuronanorobot; neuronanorobotics; whole-brain emulation.

1. Introduction

The human brain is the only body organ that cannot, even in principle, be transplanted from a donor without fundamentally altering the individual persona of the recipient. Information pertaining to brain structure, neural connectivity, neurotransmitter activity, cellular and organ-level neurological function, and higher mental states including personality and self-awareness can be permanently altered or lost as a result of physical trauma, pathogenic diseases, and a variety of common degenerative disorders such as ALS and Alzheimer's, Huntington's and Parkinson's diseases. Once destroyed, this information cannot, even in principle, be recovered using current techniques, thus permanently diminishing patient health. It must be a

key goal of future medical technology to provide novel methods for non-destructively acquiring, transmitting, validating, and archiving comprehensive brain-related structural and functional information. Such person-specific information, once preserved, might subsequently be employed to analyze existing pathologies at cellular detail and to devise appropriate therapies, and ultimately might be used to guide processes designed to restore the original state of the brain that existed prior to its pathological degradation.

The emerging prospect of medical nanorobotics [Freitas, 1998, 1999a,b, 2003, 2005a,b; Morris, 2001; Astier *et al.*, 2005; Patel *et al.*, 2006; Park *et al.*, 2007; Popov *et al.*, 2007; Martel *et al.*, 2009; Mallouk and Sen, 2009; Kostarelos, 2010; Mavroides and Ferreira, 2011] offers an ideal technology for monitoring, recording, and even manipulating many different types of brain-related information. This paper previews a proposed new medical technology called neural nanorobotics or neuronanorobotics. Medical neuronanorobots may be capable of real-time monitoring of single-neuron neuroelectric activity, local neuropeptide traffic, and other relevant functional data, and may also be able to acquire relevant structural information including neuron surface features and connectome mapping [Sporns *et al.*, 2005; Lu *et al.*, 2009; Anderson *et al.*, 2011; Kleinfeld *et al.*, 2011; Seun, 2011] in a living brain. Non-destructive whole-brain monitoring would be enabled by the coordinated activities of large numbers of cooperating neuronanorobots. When coupled with single-cell repair capabilities [Freitas, 2007], advanced medical neuronanorobotics provides the ultimate technology needed to treat Parkinson's and Alzheimer's diseases, other brain-related neurodegenerative disorders, epilepsy, dementia, memory and sensory disorders, spinal cord and neuromuscular disorders, pain and toxic disorders, and a wide variety of traumatic injuries to the brain.

The advent of medical nanorobotics requires the ability to build nanorobotic devices and to produce these devices in sufficient therapeutic quantities to treat individual patients. The most advanced medical nanorobots will likely be fabricated using diamondoid materials, as these materials provide the greatest strength, durability, and reliability in the *in vivo* environment [Freitas, 2010]. Designs for a wide variety of medical nanorobots have been proposed [Freitas, 1998, 2000, 2005c, 2006a, 2007]; Freitas and Phoenix [2002] and additional details are available elsewhere [Freitas, 2005b, 2006b, 2010]. The practical technical foundation for advanced medical nanorobotics requires answering a fundamental question: How to build diamondoid nanorobots, starting from current manufacturing technologies? The answer to this question is the main subject of an ongoing international collaboration whose principal objective is the construction of a nanofactory capable of mass-manufacture of medical diamondoid nanorobotic devices for medical treatments [Freitas and Merkle, 2006; Freitas, 2010]. Possible general methods to achieve massively parallel molecular manufacturing technologies, such as a nanofactory, have been reviewed in the literature [Freitas and Merkle, 2004], and methods for controlling individual and large numbers of medical nanorobots are also the subject of

current research [Cavalcanti and Freitas, 2003; Cavalcanti *et al.*, 2008; Freitas, 2009]. The present work assumes that these manufacturing challenges can be overcome.

An ongoing PhD thesis effort is investigating the potential feasibility of real-time non-destructive whole-brain *in vivo* monitoring of the many information channels of a human brain, in particular single-neuron electrical information, local neuropeptide traffic, and other relevant functional data. A comparison of the whole-brain data rate monitoring requirement with the theoretical capabilities of medical neuronanorobotics is the first step in assessing the viability of this future technology. The present work focuses on the electrical information channel and calculates the data rate requirements for acquiring, transmitting, and storing single-neuron electrical information from an entire human brain, summing estimates of bit rates and spiking rates for neurons in the main sub-regions of the human brain using a novel electrophysiological-based estimation procedure.

2. Neural Electrical Data Processing in the Human Brain

Previous estimates of human brain electrical data processing rates have ranged from a low of 1.48×10^{11} bits/sec to a high of 3.2×10^{29} bits/sec using a wide variety of assumptions and constraints not all of which are directly comparable, as summarized in ascending order in Table 1.

Assessing the total neural electrical data processing activity of the human brain (that neuronanorobots must monitor) requires consideration of several key issues:

- What are the relevant cellular, sub-cellular, or molecular level processing units of electrical information of the human brain? What is the contribution of each processing unit to the processing power of the human brain? If a processing unit changes its processing behavior (e.g., when synapses change their weightings), does this influence the processing capacity of the human brain? These issues are addressed in Sec. 2.1.
- What relevant information is carried in each spike train and in each action potential? Does an individual action potential waveform (having shape, height and width) carry relevant information? How much information is transmitted in the temporal pattern of each spike train? The action potential waveform and not just the temporal pattern of spikes (or the average spiking rate) should be included in any analysis of information transfer by neurons since it appears that the changing subthreshold voltage on which the action potential sits is a highly relevant biophysical signal that influences information processing in pools of neurons (e.g., background-modulated pulse code). These issues are addressed in Secs. 2.2 and 2.3.
- How many action potentials are generated per second in the human brain? How solidly grounded, in currently available experimental data, are the estimates of the average neuron spiking rates? How different are minimum, maximum, and average firing rates for neurons? How many neurons and synapses exist in the whole human

Table 1. Previous estimates of the electrical processing capacity of the whole human brain (partially adapted from [Sandberg and Bostrom, 2008]).

Author (year)	Est. processing rate of the whole human brain (bits/sec)	Key assumptions and notes
von Neumann [1958]	Whole human brain processing rate of 1.48×10^{11} bits/second [von Neumann, 1958].	von Neumann considered that all neural impulses conducted in the human brain during a human lifetime of 60 years are equivalent to 2.8×10^{20} bits.
Seitz [2007]	Whole human brain processing rate of 2×10^{18} synaptic updates/second [Seitz, 2007].	Seitz assumed between 0.5×10^{11} and 2×10^{11} neurons, between 10^3 and 10^5 synapses per neuron, and an average of 200 spikes/neuron/second.
Seitz [2007]	Whole human brain processing rate of 20×10^{15} cups (connection-updates-per-second) assuming 10^4 synapses per neuron [Seitz, 2007].	Seitz estimated the processing power of the human visual cortex. Assuming that the visual cortex had 6×10^9 neurons each firing 40 times per second, Seitz concluded that the processing capacity of the visual cortex was 240×10^9 spikes/sec. Assuming that the visual cortex had 5×10^{13} synapses (assuming ~15,000 interconnections per neuron), and assuming 40 spikes/neuron-sec, he estimated that the visual cortex would perform 2×10^{15} connection updates per second or, as he puts it, 2 Pcups (peta-connection-updates-per-sec).
Merkle [1989]	Whole human brain computational rate estimated roughly as 10^{16} synapse operations per second [Merkle, 1989].	Merkle assumed roughly 10^{15} synapses operating at about 10 impulses/second.
Merkle [1989]	Whole human brain computational rate estimated between 10^{12} and 10^{14} operations per second [Merkle, 1989].	Merkle estimated also that the retina as a whole performs about 10^{10} analog adds per second and so, multiplying this estimate by the ratio of brain size to retinal size he arrived at the estimate of 10^{12} and 10^{14} operations per second as the computational power of the human brain.
Moravec [1998]	Whole human brain computational rate ~10^{14} FLOPS [Moravec, 1989]	Moravec estimates the visual computational processing power of the human retina as being 1000 MIPS. Then, assuming a 1500 cubic centimeter human brain, explains that the human brain is approximately 100,000 times as large as the retina, thus concludes estimating that the processing power of the human brain is 100 million MIPS.
Merkle [1989]	Whole human brain computational rate estimated as 2×10^{15} synapse ops per second [Merkle, 1989].	Merkle estimated the total energy used by the brain each second, then divided it by the energy used for each basic operation to conclude that a 10 watt brain can do at most 2×10^{15} synapse operations per second. Merkle's three different estimates put the human brain raw computational power between 10^{13} and 10^{16} operations per second.

(*Continued*)

Table 1. (*Continued*)

Author (year)	Est. processing rate of the whole human brain (bits/sec)	Key assumptions and notes
Sarpeshka [1998]	Whole human brain processing rate estimated as 3.6×10^{15} synaptic operations per second [Sarpeshka, 1997, 1998].	Sarpeshka argues that there are about 2.4×10^{14} synapses in each cortex of the brain, with an average firing rate (at the cortex) of 7.5 Hz (between 5−10 Hz). He observes that he is assuming that each synapse is always operational and constantly computing. He concludes that the number of synaptic operations per second is $2 \times 2.4 \times 10^{14} \times 7.5 = 3.6 \times 10^{15}$.
Kurzweil [1999]	Whole human brain processing rate estimated as 2×10^{16} FLOPS (64×10^{16} bits/sec, assuming single-precision) [Kurzweil, 1999].	Kurzweil assumed 10^{11} neurons, 10^3 synapses per neuron and 200 operations per second. Kurzweil puts it as a "conservatively high estimate".
Dix [2005]	Whole human brain processing rate estimated as 10^{16} synaptic ops/second (or 10 peta-nuop per second; nuop = neural operations per second) [Dix, 2007].	Dix assumed 10^{10} neurons and 10^4 synaptic operations per cycle, and 100 Hz cycle time. It is worth noting that Dix calls his estimates "back of the envelope calculations".
Malickas [1996]	Whole human brain processing rate estimated between 10^{15}−10^{18} synaptic operations per second [Malickas, 1996].	Malickas observes that Merkle estimates a lower value, between 10^{13} and 10^{16} synaptic operations per second.
Bostrom [1998]	Whole human brain processing rate estimated as 10^{17} operations per second [Bostrom, 1998].	Bostrom assumed 10^{11} neurons, 5×10^3 synapses and synapses firing at 100 Hz, with each signal using 5 bits. Bostrom emphasizes that his estimate must be a maximum value given redundancy of information in the brain, and illustrates with a previous estimate from Moravec of 10^{14} FLOPS (or 32×10^{14} bits/sec). Bostrom observes that these estimates refer to what he believes is the minimal amount of computation necessary to replicate the chemical and electrodynamic features of the neuronal response function that is relevant for the total performance of the neural net. He notes that the degree of detail necessary to replicate the individual neuron and brain performance is unknown.
Fiala [2007]	Whole human brain processing rate estimated as 2.56×10^{17} bytes/second [Fiala, 2007; Sandberg and Bostrom, 2008].	Fiala seems to have assumed 10^{14} synapses, with identity coded by 48 bits plus (2×36) bits for pre- and post-synaptic neuron identity, and 1 byte for state, with a 10 ms timescale.
Sandberg [2009]	Whole human brain processing rate estimated as 1.2×10^{18} FLOPS (or 38.4×10^{18} bits/sec) [Sandberg and Bostrom, 2008].	For emulation purposes, Sandberg assumed 10^{11} neurons, each with 10^4 compartments running the Hodgkin−Huxley equations with 1200 FLOPS each. Each compartment would have four dynamical variables and 10 parameters described by one byte each.

(*Continued*)

Table 1. (*Continued*)

Author (year)	Est. processing rate of the whole human brain (bits/sec)	Key assumptions and notes
Thagard [2002]	Whole human brain processing rate estimated as $\sim 10^{23}$ (or 32×10^{23} bits/sec) FLOPS [Thagard, 2002].	Thagard speculates that the processors in the brain might be the proteins and not just the neurons. He assumes that one neuron influences 10^6 brain proteins via released hormones. Thagard argues also that the number of processors in the brain is certainly more than the 10^{11} neurons, but also notes that the processor count is probably less than 10^{17} (the number of proteins in the brain).
Hameroff [1987] and Penrose [1989]		Proposed that quantum effects may play an important role in the function of the brain and that microtubule network underlies consciousness [Hameroff, 1987; Penrose, 1989]. If each of the 10^{16} microtubules in the whole-brain neuron population stores one single qubit then the 10^{16} qubit system would require a classic computer with $20^{10,000,000,000,000,000}$ bits; if each neuron microtubule system acts as an isolated quantum computing network then the whole brain would have 10^{11} connected 100,000 qubit quantum computers [Sandberg and Bostrom, 2008].
Tuszynski [2006]	Whole human brain processing rate estimated as 10^{28} FLOPS (or 32×10^{28} bits/sec) [Tuszynski, 2006].	Assumes classical computation on microtubules. Tuszunski explains that each microtubule dimer can have 32 states (four states per dimer, four states per electron inside the tubulin dimer, with at least two computational states), and since there are 13 dimers per ring and 1250 rings per mid-size microtubule, then each microtubule would have 100 kilobytes of information. The known number of microtubules per neuron suggests 10^9 bytes per neuron, yielding 10^{19} bytes per brain assuming 10^{10} neurons per brain. If the electrons oscillate or make transitions in this state on the order of nanoseconds, then the processing power is 10^{28} FLOPS (or 32×10^{28} bits/sec).

brain? These issues are addressed using a novel electrophysiological approach in Secs. 3 and 4.

2.1. *Neural electrical information processing units*

There seems to be some disagreement on what should be considered a processing unit. A structural component, such as a neuron or a synapse, should be considered a processing unit if there are "relevant" changes to the input/output of action potentials that interacts with that structural component. A metric to measure the "relevance" of the changes is thus required. In the literature there is general

consensus that neurons and synapses should be considered as processing units, but there is no agreement about whether dendritic trees, axons, proteins, or neural microtubules should be considered as relevant processing units.

Neurons are electrical information processing units because they receive, integrate, generate, transmit and communicate information using action potentials [Koch, 1997; Koch and Segev, 2000; Zhang, 2008]. Neurons receive electrical data mostly via their dendritic tree, then integrate it in the soma. Neurons then generate new information encoded in the form of action potentials in the axon hillock and axon initial segment, transmit the action potentials through the axon, and communicate the information to the next neuron cell via its synapses. In this paper we do not attempt to quantify the functional significance of these different processing stages (dendritic tree, soma, axon and synapse) in neuronal information processing [Koch, 1983; London and Hausser, 2005; Zador, 1998; Juusola, 1996; Bialek, 1993; Manwani, 2001]. We will not attempt to quantify the neuronal noise sources and their influence on the reliability and precision of neuronal signaling [Bialek and Rieke, 1992], and we also ignore important issues like the precise quantification of the reliability of stimulus-response functions or the question of what is being encoded by spike activity.

Synapses are the key part of the neuron network that processes information and is involved in learning and memory [Xu *et al.*, 2007; Black *et al.*, 1990; Bliss and Collingridge, 1993; IBM, 2008; Holtmaat and Svoboda, 2009]. Synapse size and shape is reported to play a role both in long-term and short-term memory storage and deletion [Lee *et al.*, 2008; Kandel, 2001; Puro *et al.*, 1997]. Apart from being key elements for signal transduction and plasticity, synapses in most cases ensure one-way transmission of signals, allow more complex system behaviors, and slow down electrical signals [Rollenhagen and Lübke, 2006; Rollenhagen *et al.*, 2007]. Theoretical results have shown that the computational power of a network is increased through the use of dynamic synapses [Maas, 1999], and synapses are involved in temporal processing of information [Fuhrmann *et al.*, 2002]. The emulation of biological synapses is considered necessary as a building block for brain-like computational systems [Kuzum *et al.*, 2011]. We therefore regard synapses as the most relevant electrical processing units of the human brain.[1]

[1] For simplicity, we assume here that real-time information processing in the brain can be monitored by placing one neuronanorobot at each synaptic connection in the brain and having it record/transmit data on spiking at this local synapse, though other approaches may also be considered. It is possible that this method of collecting data might provide redundant information since thousands of synapses share a common spiking neuron, in which case the present analysis provides an upper limit to the data processing requirements of a network of nanorobots placed one per synapse, which could overestimate the overall information processing capacity of the brain. But while some synapses have a common spiking neuron, synapses are the processing units of electrical information and do not generate action potentials but instead process electrical signals, which is why measuring the spikes produced by neurons is not enough to quantify the electrical information being processed in the human brain.

2.2. *Information content of individual action potential waveform*

Various types of neurons have differences in the shape, rate, and pattern of firing of action potentials [Bean, 2007; Brenner, 2000]. Action potentials encode information in their shape, or waveform [Bean, 2007; Polavieja *et al.*, 2005]. Small differences in action potential waveform can produce changes in the timing of presynaptic calcium entry, leading to dramatic changes in the postsynaptic response [Bean, 2007]. The "typical" $\sim$20 μm human neuron discharges 5−100 action potentials per second, moving from approximately −65 mV potential to approximately +35 mV potential in $\sim 10^{-3}$ sec. More specifically, the rising phase of an action potential reaches its peak of +38.9 mV in $\sim$0.592 ms in unmyelinated axons, then repolarizes and crosses −65 mV at 1.3 ms after the peak, after reaching maximum hyperpolarization of −77 mV at 1.261 ms after the peak [Crotty *et al.*, 2006].

The action potential is a localized change in Na^+ and K^+ ion concentrations and the action potential waveform depends on small changes in the timing of the Na^+ and K^+ influx and efflux. Experimental data reports a "typical" action potential having the first peak of the Na^+ current occurring 100 μs before the peak of the action potential at a magnitude of 943 $\mu A/cm^2$ per unit axon surface area [Crotty *et al.*, 2006]. The falling Na^+ current, at a magnitude of 35 $\mu A/cm^2$, reaches equality with the rising potassium current 50 μs after the voltage peak, after which the Na^+ current rises to a second peak of 417 $\mu A/cm^2$ at 150 μs after the action potential peak [Crotty *et al.*, 2006]. From this second peak, the Na^+ current then declines over a period of about half a millisecond, approaching its rest value of 4 $\mu A/cm^2$ [Crotty *et al.*, 2006]. In the action potential the period of the net inward Na^+ flux has a value of 0.108 $\mu C/cm^2$, which gives a flux per unit axon length of 16 nC/cm or an energy cost of 4.2 nJ/cm [Crotty *et al.*, 2006]. The K^+ current has only a single peak, which occurs 225 μs after the action potential peak at a magnitude of 621 $\mu A/cm^2$. The net K^+ flux has a value of 0.107 $\mu C/cm^2$ [Crotty *et al.*, 2006].

Action potentials are initiated not only at the axon hillock but also at the axon initial segments ($\sim$35 μm from the axon hillock) and even at the first node of Ranvier ($\sim$90 μm from the axon hillock) [Palmer and Stuart, 2006; Palay *et al.*, 1968]. For example, in some pyramidal neurons of cortical layer five, action potentials are initiated at the axon initial segment [Palmer and Stuart, 2006]. The axon initial segment molecular organization includes high densities of specialized protein complexes consisting of ion channels, CAMs, cytoskeletal and scaffolding proteins, and modulatory proteins [Ogawa and Rasband, 2008]. Among this molecular variety, the axon initial segment Kv1 potassium channels (which have a 10-fold increase in the first 50 μm of the axon initial segment) control both axonal action potential waveform and synaptic efficacy [Kole *et al.*, 2007]. Kv1 potassium channels shape the action potential waveform in the axon initial segment of layer 5 pyramidal neurons, independent of the soma [Kole *et al.*, 2007].

Action potentials carry information (which depends on the previous 50 ms of conductance stimulus history) in their waveform [Polavieja *et al.*, 2005; Bean, 2007].

The rate of information transfer considering only action potential waveforms is estimated to be 3−4 times larger than that of the stereotyped spike train impulses (considering only the spike timing pattern) [Polavieja *et al.*, 2005]. In one example, at a spike rate of 10 Hz the spike train transmits ∼200 bits/sec whereas the stereotyped impulses transmit only ∼50 bits/sec [Polavieja *et al.*, 2005]. Since the remaining 150 bits/sec are encoded in the action potential waveform, then at a firing rate of 10 Hz the average number of bits[2] encoded on each action potential waveform is estimated as ∼15 bits/spike.

2.3. *Information content of spike train pattern*

The average quantity of information encoded in each spike comprising a spike train temporal pattern (not considering the information contained in an action potential waveform; Sec. 2.2) is variously estimated to lie between 0.01−10 bits/spike, a rather wide range.

More specifically, the information transmitted by cells in the retina and inferior temporal cortex in response to constant stimuli is estimated to be on the order of ∼0.01 bits/spike [Buracas and Albright, 1999]. Neurons in monkey cortex are estimated to carry <0.1 bits/spike [Buracas and Albright, 1999], whereas the average neocortical spike carries about 0.01−0.2 bits/spike with some neocortical neuron spikes carrying 0.5−2 bits/spike [Buracas and Albright, 1999]. Individual neuronal spikes in spike trains from some sensory systems convey in the range of 1−3 bits/spike of information about the stimulus that triggered them [Buracas and Albright, 1999] and similar estimates of 1−3 bits/spike are reported for a wide variety of systems [Buracas and Albright, 1999]. Estimates using information-theoretic analysis of monkey visual system neurons yield information transmit rates of ∼1.5 bits/spike during a spike train [Borst and Theunissen, 1999] with the general average information per spike estimated at 2−3 bits/spike [Rieke *et al.*, 1997]. Studies of target-selective descending neuron spikes of the dragonfly report ∼4 bits/spike [Adelman *et al.*, 2003] and ∼1.5 bits/spike [Adelman *et al.*, 2003], and another study [Rieke *et al.*, 1997] finds that sensory spikes can carry between 1−10 bits/spike of information. The quantity of entropy[3] encoded in each spike of a spike train (considering only the spike train temporal pattern) is reported to vary with the firing rates, from 8 bits/spike for ∼3 Hz firing rates down to ∼3 bits/spike for ∼100 Hz firing rates (Fig. 1) [Zador, 1998]. Figure 2 shows the quantity of information, entropy, and conditional entropy[4] processed per second as a function of firing rate [Zador, 1998].

[2] "Information" can be defined as: facts, data, or instructions in any medium or form. Mathematically, "information" is defined as a numerical measure of the uncertainty of an experimental outcome. Information is usually measured in binary digits or "bits". A bit is defined as a fundamental unit of information having two possible values, 0 or 1. A bit can also be defined as a measure of the reduction of uncertainty, with one bit corresponding to a reduction of uncertainty by a factor of two.

[3] In this context, entropy (or Shannon entropy) quantifies the total output variability of a spike train.

[4] Conditional entropy quantifies the variability that remains when the input signal is held constant. Information (or mutual information) quantifies the difference between entropy and conditional entropy.

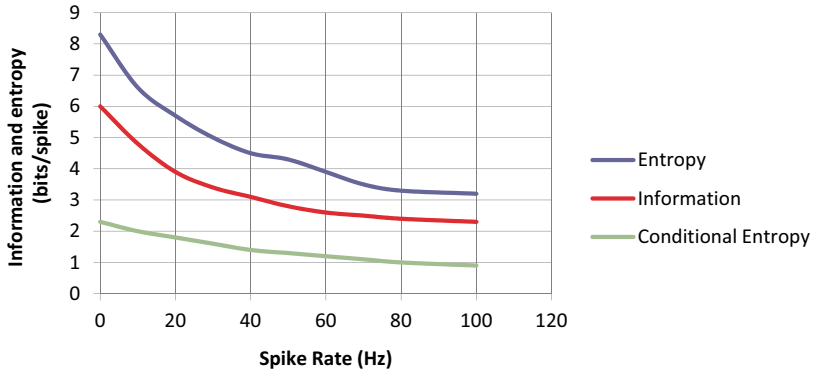

Fig. 1. Quantity of average information transmitted by each spike of a spike train (considering only spike train temporal pattern) as a function of firing rate (adapted from [Zador, 1998]).

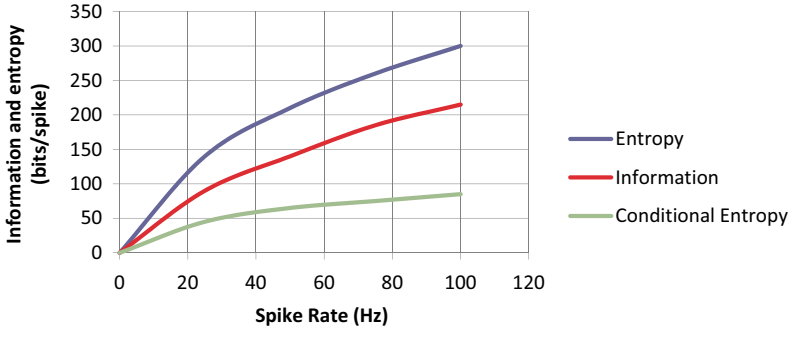

Fig. 2. Quantity of average information transmitted in a spike train temporal pattern as a function of firing rate (adapted from [Zador, 1998]).

Summing the information carried in the spike train temporal pattern and the information encoded in each individual spike waveform, the average quantity of information transmitted per spike in neuro-electrical communication depends on the neuron average firing rate (Sec. 3) and is 3−4 times larger than the information transmitted in a spike train temporal pattern, thus varies between about 6−24 bits/spike.

3. Estimating Spike Rate Using an Electrophysiological Approach

Neural spikes are produced in neurons at the axon hillock-initial segment [Eccles, 1957; Colbert and Johnston, 1996; Stuart and Sakmann, 1994]. Different types of neurons have different minimum, maximum, and average spike firing rates. Neurons can be catalogued using a wide variety of characteristics such as neuron location, morphology of neuron dendritic somatic or axonic processes, neuron receptive field characteristics, axon conduction velocity, neurotransmitter content and receptors,

intrinsic electrophysiological properties, and many other morphological or physiological characteristics. An estimate of the number of spikes generated in a whole human brain could be produced if neurons can be catalogued into groups having characteristic firing rates.

The first classification strategy for neurons focused on morphological characteristics. Some have argued that neuron morphological types do not have characteristic firing rates [Markram, 1998], and in fact most morphological types seem to have a very broad range of firing rates and patterns [Markram, 1998]. The inability to discriminate electrophysiological neuron types in different morphological categories was reported for rat cortical regions [Hamam *et al.*, 2000; Weiss and Veh, 2011; Hamam *et al.*, 2002; McGann *et al.*, 2001; Staiger *et al.*, 2004], rat amygdala [Faulkner and Brown, 1999], and the rat dorsal nucleus of the lateral lemniscus [Wu and Kelly, 1995]. On the other hand, although there is no mutual correspondence between neuron morphological categories and neuron firing rates, it is also known that structural factors influence neuron electrophysiological features. For example, neurons with the same channel densities and anatomical size can have functional differentiation caused by distinctions in dendritic topology [Duijnhouwer *et al.*, 2001]. Also, the morphology of dendrites may affect pyramidal neuron cell physiology such as electrotonic properties, action potential back-propagation, firing patterns, synaptic integration, and coincidence detection [Scorcioni *et al.*, 2004; Zachary, 1996]. There is a large number of morphological dendritic parameters that are used to characterize dendritic morphology and that can have some degree of impact on neuron electrophysiological features. Several studies confirm a correlation between morphological characteristics and some physiological properties [Connors *et al.*, 1982; Hestrin and Armstrong, 1996; Cauli *et al.*, 1997; Nambu and Llinas, 1997; Takakusaki *et al.*, 1997; Allers and Sharp, 2003; Kuwana *et al.*, 2006; Lee *et al.*, 2007] but to the best of our knowledge no current study presents the typical firing rates for each morphological type of neuron.

Apart from morphological classification, neurons can also be catalogued directly according to firing pattern, giving origin to different electrophysiological classes of neurons (16 different classes and subclasses). The different electrophysiological types of neurons seem to have characteristic average, minimum, and maximum firing rates [Diego, 2004], with different human brain regions possessing different percentages of each neuron electrophysiological type. This suggests that a useful strategy for estimating the whole-brain spike rate may be to quantify the number of neurons of each electrophysiological type. Neuron electrophysiological characteristics are very likely grounded in morphological features but to the best of our knowledge there is currently no study revealing the exact structural correlates of the various electrophysiological classes. In this work, we consider the three main electrophysiological types of neurons in the human brain: Regular Spiking (RS), Fast Spiking (FS), and Bursting (B) [Diego, 2004; Steriade, 2004]. Each of these three electrophysiological classes has several subclasses (e.g., intrinsically bursting or fast repetitive bursting,

aka. chattering), but most such details are beyond the scope of this paper. There are also other electrophysiological neuron types such as late-spiking, low-threshold spiking, and single-spiking, but these are apparently few in number in the human brain and thus will be ignored in the present analysis.

Qualitatively, the three main electrophysiological types of neurons have several main differences. RS cells fire at low rates and adapt to continuous stimuli, while FS cells sustain very high firing frequencies with little or no adaptation and B cells generate clusters of spikes either singly or repetitively [Barry and Gutnickb, 1990]. RS and FS electrophysiological types reflect the intensity of the input in their firing frequency in linear proportion, whereas the frequency-intensity curve (response-stimulus) of B cells is highly nonlinear [Diego, 2004].

Quantitatively, RS cells respond to a "typical" depolarizing stimulus of 0.3 nA with initial frequencies of 100 Hz in the first 2 ms, then accommodate during the following 50 ms to steady frequencies of about 30 Hz (usually range 20−50 Hz) [Diego, 2004; Wilson, 1999]. RS firing frequencies can rise to 200−300 Hz [Diego, 2004] with each spike lasting for ∼1 ms [Diego, 2004]. An FS cell responds to a depolarizing stimulus of 0.3 nA with a sustained high frequency of 250−350 Hz (though discharges can sometimes reach the 400−800 Hz range) [Diego, 2004; Wilson, 1999]. The duration of FS spikes is usually 0.4−0.6 ms. A B cell responds to a depolarizing stimulus of 0.3 nA with a repetitive burst discharge, with an intraburst frequency of 300 Hz (the first burst might reach 600 Hz) and an interburst frequency of 40 Hz [Steriade, 2004]. B neuron high-frequency (300−600 Hz) spike bursts recur at fast rates (30−50 Hz) within a certain range of membrane potentials [Steriade, 2004; Wilson, 1999; Steriade *et al.*, 1998; Wang, 1999]. Bursting neurons have two main subtypes (intrinsically bursting (IB) and fast-repetitive bursting (FRB)) having significant differences: During sustained depolarization, IB neurons fire a short burst of 3−5 action potentials at ∼200 Hz [Diego, 2004] which becomes repetitive usually at frequencies around 5−15 Hz [Diego, 2004]. During sustained depolarization, FRB neurons fire bursts containing 25 spikes at frequencies from 200−600 Hz, with short spikes of ∼0.6 ms [Diego, 2004] bursts repeating regularly at 20−80 Hz [Diego, 2004].

Estimates of average firing rates indicate that FS neurons have the highest firing rates, followed by B and then RS cells [Diego, 2004]. Assuming appropriate stimulation, Fast-Spiking cells might achieve average firing rates of 45−55 Hz, Bursting cells 25−35 Hz, and Regular-Spiking cells 5−10 Hz [Diego, 2004], although there are reports of somewhat smaller mean values [Steriade *et al.*, 2001].

To better understand the variability around the average firing rates of the different electrophysiological types of neurons we will quantify the average firing rates during three different mental states (wake, Slow-Wave Sleep (SWS), and REM sleep) and the different firing rates for each electrophysiological neuron type while in the two principal neuron activation states (excited or resting).

The mean firing rates of the three main electrophysiological neuron types show significant differences during the three behavioral states [Steriade *et al.*, 2001].

During the state of waking, neurons of electrophysiological type RS, B and FS have average firing rates of 9.4 ± 1.7, 15.0 ± 2.5, and 23.7 ± 6.1 Hz, respectively [Steriade *et al.*, 2001]. During SWS the three neuron types discharged respectively at 11.8 ± 1.6, 7.5 ± 1.9, and 14.9 ± 4.1 Hz [Steriade *et al.*, 2001], while the three neuron types discharged respectively at 14.0 ± 2.8, 5.4 ± 2.4 and 30.6 ± 8.4 Hz during REM sleep [Steriade *et al.*, 2001].

Electrophysiological neuron types can also be found in either an excited or a resting activation state. When excited the average spike rates of each electrophysiological type varies mainly with the depolarized resting membrane potential (V_m) [Diego, 2004] or current intensity [Lionel *et al.*, 2003]. Increases in the V_m of the waking state changes completely the average firing rates [Diego, 2004]. There is a linear relationship between V_m and neuron spike rate, with differences in slope: FS cells have the steepest slope at 9.2 Hz/mV, followed by B cells at 4−8 Hz/mV and RS cells with ∼1 Hz/mV [Diego, 2004].

The spontaneous firing rates of different morphological and electrophysiological neuronal types are diverse and vary between 0−40 Hz. Let us consider some examples of that variability. Cat neocortical neurons generate and synchronize a slow oscillation at 0.5−1 Hz [Steriade *et al.*, 2001]. Histaminergic and aminergic neuron populations display a slow regular firing pattern at 1−4 Hz in the absence of synaptic activation [Haas, 2008]. The spontaneous firing rates of basolateral amygdala projection cells average 2.1 ± 0.4 Hz (ranging from 0−16 Hz, with nearly 51.2% of projection cells firing ≤1 Hz and with an important subset firing at higher rates, up to 6.8 Hz). Neurons with unusually high spontaneous firing rates of 9−16 Hz are also observed [Likhtik *et al.*, 2006]. Spontaneous discharge of pallidal neurons is reported in the 3−19 Hz range [Raz *et al.*, 2000; Wilson, 1981]. In human brains, fast oscillations are reported at 30−40 Hz while awake and at REM sleep but at 1−4 Hz in SWS [Steriade *et al.*, 1998; Llinas and Ribary, 1993].

In the resting state, different electrophysiological neuron types have different average spontaneous firing rates. RS neurons have an estimated average resting firing rate of 5 ± 5.5 spikes/sec [Wilson *et al.*, 1994]. FS neurons have reported average firing rates between 16.1 ± 3.4 spikes/sec [Plenz and Kitai, 1998] and 17 ± 10.8 spikes/sec [Wilson *et al.*, 1994]. B neurons display spontaneously generated bursts of three to six action potentials with an interburst frequency of 0.2−4 Hz; spontaneously generated bursts of 2−10 Hz were observed just prior to the switch to the tonic-firing mode [Wang and McCormick, 1993].

4. Electrophysiological-Based Estimate of Whole-Brain Electrical Data Rate

The human brain is estimated to have $(86.06 \pm 8.2) \times 10^9$ neurons, with 80.2% or $(69.03 \pm 6.65) \times 10^9$ neurons located in the cerebellum and 19% of those neurons or $(16.34 \pm 2.17) \times 10^9$ neurons located in the cerebral cortex, with only 0.8% or $(0.69 \pm 0.12) \times 10^9$ neurons in the rest of the brain [Azevedo *et al.*, 2009]. The human

cerebellum and cerebral cortex together hold the vast majority (99.2%) of the number of neurons of the whole human brain [Azevedo *et al.*, 2009]. The synaptic information processing rate for the brain may be estimated as:

$$T_{ss}(\text{spikes/sec}) = \sum_i \left[\frac{(F_{rs} \times RS_i) + (F_b \times B_i) + (F_{fs} \times FS_i)}{n_i} \right] \times s_i \qquad (1)^5$$

and as:

$$T_{sb}(\text{bits/sec}) = 3.5 \times \sum_i \left[\frac{\begin{array}{c}(f(F_{rs}) \times F_{rs} \times RS_i) + (f(F_b) \times F_b \times B_i) \\ + (f(F_{fs}) \times F_{fs} \times FS_i)\end{array}}{n_i} \right] \times s_i \qquad (2)^5$$

where: T_{ss} = whole-brain number of synaptic processed spikes per second; F_{rs} = average firing rate of RS neurons; RS_i = number of RS neurons of brain region "i"; F_b = average firing rate of B neurons; B_i = number of B neurons of brain region "i"; F_{fs} = average firing rate of FS neurons; FS_i = number of FS neurons of brain region "i"; n_i = total number of neurons in brain region "i"; s_i = total number of synapses in brain region "i"; f represents the function of information (Fig. 2); and T_{sb} = whole-brain number of synaptic processed bits per second.

Experimental quantitative data on the number of neurons and the number of synapses within each main region of the human brain, along with the percentages of electrophysiological neuron types in each of those brain regions, are compiled in Table 2. Some of this data is incomplete and must be crudely estimated, pointing to the need for additional experimental efforts, but the error in the final total should be relatively small because the most populous neural subregions are comparatively well-studied — the single largest likely source of remaining error appears to be in our estimate of the number of synapses in the human cerebellum. These data may be combined using Eqs. (1) and (2) to yield an estimate of the synaptic-processed spike rate of $T_{ss} = (4.31 \pm 0.86) \times 10^{15}$ spikes/sec and the synaptic-processed bit rate of $T_{sb} = (5.52 \pm 1.13) \times 10^{16}$ bits/sec for the entire human brain.

These results for the quantity of electrical information processed in the whole human brain are very roughly in accord with previous estimates by Seitz, Merkle, Kurzweil, Malickas, Dix, and Fiala, but diverge significantly from estimates by Thagard, Hameroff and Tuszinsky mostly because these latter authors consider proteins and microtubules to be the relevant information processing units rather than neurons and synapses.

Note that T_{ss} is the maximum event detection requirement for the entire embedded *in vivo* sensor system in the context of nanorobotic whole-brain monitoring. With population coding — an idea based on cortical lateral connections that has been used to implement an "ideal observer", that is, an optimal decoding of

[5]Even distribution of synapses among the different electrophysiological types of neurons is assumed in Eqs. (1) and (2).

Table 2. Electrical data processing in the human brain.

Region/Subregion (level 1)	Subregion (level 2)	Number of neurons	Percentages of RS neurons	Percentages of B neurons	Percentages of FS neurons	Total number of synapses	Total electrically processed spikes/sec and bits/sec
Forebrain							
Forebrain/Telencephalon							
	Cerebral Cortex	$(2.09 \pm 0.42) \times 10^{10}$ (10) (3)	54% [Steriade *et al.*, 1998] (1)	43% [Steriade *et al.*, 1998] (2)	3% [Steriade *et al.*, 1998] (4)	$(1.64 \pm 0.26) \times 10^{14}$ [Tang *et al.*, 2001, 2003] (6) (20)	$(3.03 \pm 0.48) \times 10^{15}$ spikes/sec, $(3.92 \pm 0.63) \times 10^{16}$ bits/sec (7)
	Cerebral Cortex/ Frontal Lobe	$(6.70 \pm 1.41) \times 10^{9}$ [Pedersen, 2005] (11)	95% [Chang and Luebke, 2007]	5% [Chang and Luebke, 2007]	0% [Chang and Luebke, 2007]	$(5.85 \pm 1.34) \times 10^{13}$ [Tang *et al.*, 2001, 2003] (20)	$(5.05 \pm 1.16) \times 10^{14}$ spikes/sec, $(8.34 \pm 1.91) \times 10^{15}$ bits/sec
	Cerebral Cortex/ Insula	$(8.72 \pm 0.33) \times 10^{8}$ (est.) (8)	54% [Steriade *et al.*, 1998] (1) (21)	43% [Steriade *et al.*, 1998] (2) (21)	3% [Steriade *et al.*, 1998] (4) (21)	$(6.05 \pm 0.23) \times 10^{12}$ (est.) (8)	$(1.12 \pm 0.04) \times 10^{14}$ spikes/sec, $(1.45 \pm 0.05) \times 10^{15}$ bits/sec
	Cerebral Cortex/ Limbic Lobe	$(1.39 \pm 0.30) \times 10^{9}$ (9)	82% [Tavares, 2006]	16% [Tavares, 2006]	2% [Tavares, 2006]	$(4.00 \pm 1.05) \times 10^{13}$ synapses (est.) (9)	$(4.78 \pm 1.25) \times 10^{14}$ spikes/sec, $(6.98 \pm 1.83) \times 10^{15}$ bits/sec
	Cerebral Cortex/ Occipital Lobe	$(4.10 \pm 0.99) \times 10^{9}$ [Pedersen, 2005] (12)	54% [Steriade *et al.*, 1998] (1) (21)	43% [Steriade *et al.*, 1998] (2) (21)	3% [Steriade *et al.*, 1998] (4) (21)	$2.20 \pm 1.83 \times 10^{13}$ [Tang *et al.*, 2001, 2003] (20)	$(4.06 \pm 3.38) \times 10^{14}$ spikes/sec, $(5.26 \pm 4.38) \times 10^{15}$ bits/sec
	Cerebral Cortex/ Parietal Lobe	$(4.20 \pm 0.92) \times 10^{9}$ [Pedersen, 2005] (13)	54% [Steriade *et al.*, 1998] (1) (21)	43% [Steriade *et al.*, 1998] (2) (21)	3% [Steriade *et al.*, 1998] (4) (21)	$(4.15 \pm 0.568) \times 10^{13}$ [Tang *et al.*, 2001, 2003] (20)	$(7.66 \pm 1.04) \times 10^{14}$ spikes/sec, $(9.92 \pm 1.36) \times 10^{15}$ bits/sec
	Cerebral Cortex/ Temporal Lobe	$(3.60 \pm 0.50) \times 10^{9}$ [Pedersen, 2005] (14)	61% [Avoli, 1994] (24)	36% [Avoli, 1994] (24)	3% [Steriade *et al.*, 1998] (4) (21)	$(4.20 \pm 1.35) \times 10^{13}$ [Tang *et al.*, 2001, 2003] (20)	$(7.09 \pm 2.28) \times 10^{14}$ spikes/sec, $(9.38 \pm 3.01) \times 10^{15}$ bits/sec

(*Continued*)

Table 2. (*Continued*)

Region/Subregion (level 1)	Subregion (level 2)	Number of neurons	Percentages of RS neurons	Percentages of B neurons	Percentages of FS neurons	Total number of synapses	Total electrically processed spikes/sec and bits/sec
	Cerebral Nuclei/ Amygdala	$(1.22 \pm 0.13) \times 10^7$ [Schumann and Amaral, 2005] (15)	92% [Faber *et al.*, 2001]	1% [Faber *et al.*, 2001]	7% [Faber *et al.*, 2001]	$(8.47 \pm 0.90) \times 10^{10}$ (est.) (22)	$(9.06 \pm 0.96) \times 10^{12}$ spikes/sec, $(1.34 \pm 0.14) \times 10^{13}$ bits/sec
	Cerebral Nuclei/ Anterior Olfactory Nucleus	1.76×10^8 (18) (33)	54% [Steriade *et al.*, 1998] (1) (21)	43% [Steriade *et al.*, 1998] (2) (21)	3% [Steriade *et al.*, 1998] (4) (21)	$(1.22 \pm 0.20) \times 10^{12}$ (33)	$(2.25 \pm 0.37) \times 10^{13}$ spikes/sec, $(2.91 \pm 0.48) \times 10^{14}$ bits/sec
	Cerebral Nuclei/ Basal Forebrain	1.58×10^9 (33)	52% [Pang *et al.*, 1998] (est.)	20% [Pang *et al.*, 1998] (est.)	28% [Pang *et al.*, 1998] (est.)	$(1.10 \pm 0.18) \times 10^{13}$ (33)	$(2.63 \pm 0.43) \times 10^{14}$ spikes/sec, $(3.05 \pm 0.50) \times 10^{15}$ bits/sec
	Cerebral Nuclei/ Basal Ganglia	$(4.15 \pm 0.99) \times 10^8$ [Karlsen and Pakkenberg, 2011]	54% [Steriade *et al.*, 1998] (1) (21)	43% [Steriade *et al.*, 1998] (2) (21)	3% [Steriade *et al.*, 1998] (4) (21)	$(2.88 \pm 0.69) \times 10^{12}$ (31)	$(5.31 \pm 1.27) \times 10^{13}$ spikes/sec, $(6.89 \pm 1.65) \times 10^{14}$ bits/sec
	Cerebral Nuclei/ Claustrum	6.50×10^7 (32)	54% [Steriade *et al.*, 1998] (1) (21)	43% [Steriade *et al.*, 1998] (2) (21)	3% [Steriade *et al.*, 1998] (4) (21)	$(4.51 \pm 0.72) \times 10^{11}$ (32)	$(8.32 \pm 1.33) \times 10^{12}$ spikes/sec, $(1.08 \pm 0.17) \times 10^{14}$ bits/sec
Forebrain/ Diencephalon							
	Thalamus	7.88×10^6 [Kreczmanski, 2007] (16)	38.8% (21)	30.9% (21)	28% [Steriade *et al.*, 1998]	$(5.47 \pm 0.87) \times 10^{10}$ (est.) (16)	$(1.43 \pm 0.23) \times 10^{12}$ spikes/sec, $(1.63 \pm 0.26) \times 10^{13}$ bits/sec
	Hypothalamus	$(2.02 \pm 0.47) \times 10^8$ (est.) (27)	66% (est.)	30% [Tasker and Dudek, 1991] (25)	4% (est.)	$(4.42 \pm 0.24) \times 10^{12}$ (est.) (27)	$(6.85 \pm 0.37) \times 10^{13}$ spikes/sec, $(9.08 \pm 0.49) \times 10^{14}$ bits/sec

(*Continued*)

Table 2. (*Continued*)

Region/Subregion (level 1)	Subregion (level 2)	Number of neurons	Percentages of RS neurons	Percentages of B neurons	Percentages of FS neurons	Total number of synapses	Total electrically processed spikes/sec and bits/sec
	Epithalamus	6.96×10^7 (32)	80% [Weiss and Veh, 2011]	8% [Weiss and Veh, 2011]	12% (est.)	$(4.83 \pm 0.77) \times 10^{11}$ (32)	$(6.95 \pm 1.11) \times 10^{12}$ spikes/sec, $(9.29 \pm 1.48) \times 10^{13}$ bits/sec
	Subthalamus	5.61×10^5 (26)	49% [Beurrier *et al.*, 1999] (23)	46% [Beurrier *et al.*, 1999] (23)	5% [Beurrier *et al.*, 1999] (23)	$(3.89 \pm 0.62) \times 10^9$ (26)	$(7.77 \pm 1.24) \times 10^{10}$ spikes/sec, $(9.84 \pm 1.57) \times 10^{11}$ bits/sec
Midbrain							
Midbrain/Mesencephalon							
	Midbrain Tectum	1.54×10^8 (est.) (29)	54% [Steriade *et al.*, 1998] (1) (21)	43% [Steriade *et al.*, 1998] (2) (21)	3% [Steriade *et al.*, 1998] (4) (21)	$(1.07 \pm 0.17) \times 10^{12}$ (est.) (29)	$(1.97 \pm 0.31) \times 10^{13}$ spikes/sec, $(2.56 \pm 0.40) \times 10^{14}$ bits/sec
	Midbrain Tegmentum	1.54×10^8 (est.) (29)	54% [Steriade *et al.*, 1998] (1) (21)	43% [Steriade *et al.*, 1998] (2) (21)	3% [Steriade *et al.*, 1998] (4) (21)	$(1.07 \pm 0.17) \times 10^{12}$ (est.) (29)	$(1.97 \pm 0.31) \times 10^{13}$ spikes/sec, $(2.56 \pm 0.40) \times 10^{14}$ bits/sec
	Pretectal Region	1.54×10^8 (est.) (29)	54% [Steriade *et al.*, 1998] (1) (21)	43% [Steriade *et al.*, 1998] (2) (21)	3% [Steriade *et al.*, 1998] (4) (21)	$(1.07 \pm 0.17) \times 10^{12}$ (est.) (29)	$(1.97 \pm 0.31) \times 10^{13}$ spikes/sec, $(2.56 \pm 0.40) \times 10^{14}$ bits/sec
Hindbrain							
Hindbrain/Metencephalon							
	Pons	$(9.63 \pm 2.12) \times 10^8$ (est.) (30)	54% [Steriade *et al.*, 1998] (1) (21)	43% [Steriade *et al.*, 1998] (2) (21)	3% [Steriade *et al.*, 1998] (4) (21)	$(6.68 \pm 1.06) \times 10^{12}$ (30)	$(1.23 \pm 0.20) \times 10^{14}$ spikes/sec, $(1.60 \pm 0.25) \times 10^{15}$ bits/sec

(*Continued*)

Table 2. (*Continued*)

Region/Subregion (level 1)	Subregion (level 2)	Number of neurons	Percentages of RS neurons	Percentages of B neurons	Percentages of FS neurons	Total number of synapses	Total electrically processed spikes/sec and bits/sec
	Cerebellum	$(6.903 \pm 0.665) \times 10^{10}$ [Azevedo *et al.*, 2009] (17)	54% [Steriade *et al.*, 1998] (1) (21)	43% [Steriade *et al.*, 1998] (2) (21)	3% [Steriade *et al.*, 1998] (4) (21)	$3.35 \pm 1.54 \times 10^{13}$ (19)	$(6.28 \pm 2.84) \times 10^{14}$ spikes/sec, $(8.01 \pm 3.68) \times 10^{15}$ bits/sec
Hindbrain/Myelencephalon							
	Medulla Oblongata	$(2.87 \pm 0.63) \times 10^{8}$ (est.) (28)	54% [Steriade *et al.*, 1998] (1) (21)	43% [Steriade *et al.*, 1998] (2) (21)	3% [Steriade *et al.*, 1998] (4) (21)	$(1.99 \pm 0.32) \times 10^{12}$ (est.) (28)	$(3.67 \pm 0.59) \times 10^{13}$ spikes/sec, $(4.76 \pm 0.76) \times 10^{14}$ bits/sec
Total	**Total**	$(9.42 \pm 1.13) \times 10^{10}$	54% (est.)	43% (est.)	3% (est.)	$(2.42 \pm 0.29) \times 10^{14}$	$(4.31 \pm 0.86) \times 10^{15}$ spikes/sec, $(5.52 \pm 1.13) \times 10^{16}$ bits/sec

Notes: (1) Reported range is 51%−73% [Steriade *et al.*, 1998, 2001; Foehring, 1990; Franceschetti *et al.*, 1995].
(2) The 43% is divided as 28% FRB and 15% IB [Steriade *et al.*, 1998]. The total percentage of bursting neurons ranges from: 4%−43% [Steriade *et al.*, 1998, 2001].
(3) Estimates of the number of neocortical neurons include: 17.8×10^9 [Karlsen and Pakkenberg, 2011], 20.5×10^9 (CV = 0.13) [Bundgaard, 2001], 21.2×10^9 [Pelvig *et al.*, 2003], 22.06×10^9 [Pakkenberg, 1993], 23×10^9 [Pakkenberg and Gundersen, 1997; Schumann and Amaral, 2005], 24.4×10^9 [Fischer, 1999] and $\sim 28 \times 10^9$ neurons [Wilson, 1999]. The total number of neocortical neurons in the right hemisphere of five normal 80-year-old men was estimated to be 13.7×10^9 with an inter-individual coefficient of variation of 12% [Braendgaard *et al.*, 1990]. Gender differences are illustrated on the estimate of 22.9×10^9 for males and 19.7×10^9 for females [Scorcioni *et al.*, 2004]. To illustrate the differences between healthy and disease states, the number of neocortex neurons was estimated as 24.4×10^9 in healthy individuals and 18.3×10^9 in AIDS patients [Fischer, 1999]. The number of neurons in the neocortex also changes with gender and height [Pakkenberg and Gundersen, 1997]. The range of neocortical number of neurons is reported in the range of 14.7×10^9 to 32.0×10^9, with mean values of 19.3×10^9 and 22.8×10^9 for females and males, respectively [Pakkenberg and Gundersen, 1997].
(4) Reported range is 3−24% [Steriade *et al.*, 1998, 2001].
(5) Some have reported that the cerebral cortex synaptic density is between $15.08 \times 10^8/\text{mm}^3$ and $16.26 \times 10^8/\text{mm}^3$ [deFelipe, 1999]. The numerical density of synapses in the six layers of the human cerebral cortex is reported between $10-20 \times 10^8/\text{mm}^3$ [deFelipe, 1999]. The frontal cerebral cortex numerical synaptic density was reportedly constant throughout adult human life (ages 16−72 years) with a mean of 11.05×10^8 synapses/mm^3 (±0.41 S.E.M), but there is a slight decline in synaptic density in the brains of humans aged 74−90 years with a mean of 9.56×10^8 synapses/mm^3 (±0.28 S.E.M.) [Huttenlocher, 1979].
(6) Others have estimated 1.5×10^{14} [Pakkenberg, 2003].

(*Continued*)

Table 2. (*Continued*)

(7) T_{SS} (spikes/sec) = [((7.5 spikes/sec × (1.02 × 10^{10}) neurons +30 spikes/sec × (0.81 × 10^{10}) neurons +50 spikes/sec × (0.056 × 10^{10}) neurons)/1.88 × 10^{10}) × (1.64 × 10^{14}) synapses] = 3.03 × 10^{15} spikes/sec. T_{SB} (bits/sec) = 3.5 × [((5 bits × 7.5 spikes/sec × (1.02 × 10^{10}) neurons +3.4 bits × 30 spikes/sec × (0.81 × 10^{10}) neurons +2.8 bits × 50 spikes/sec × (0.056 × 10^{10}) neurons)/1.88 × 10^{10}) × (1.64 × 10^{14}) synapses] = 5.712 × 10^{16} bits/sec.
(8) The insula has two portions: the anterior insula (larger) and the posterior insula (smaller) [Türe *et al.*, 1999]. The anterior insular cortex volume is: 3800 mm^3 (SD = 420) (left) and 3550 mm^3 (SD = 332) (right). The posterior insular cortex volume is: 1992 mm^3 (SD = 245) (left) and 1916 mm^3 (SD = 223) (right) [Nishida *et al.*, 2011]. The total volume of the human insula is thus 11,258 mm^3. Assuming a synaptic density of 11.05 × 10^8/mm^3 (average synaptic density reported for the neocortex [Huttenlocher, 1979]), the insula would have 1.24 × 10^{13} synapses. The volume of the insula is estimated as: 17.3 ± 1.9 cm^3 [Kennedy *et al.*, 1998]. As the neocortex neuron density was estimated as 50.4 × 10^6/cm^3 ± 11.08 × 10^6 (CV = 0.22) [Bundgaard, 2001], we estimate the number of neurons of the human insula as (8.72 ± 0.33) × 10^8 neurons. Assuming an average of 6.94 × 10^3 synapses per neuron (as in the human cerebral cortex [Tang *et al.*, 2003]), the insula would have (6.05 ± 0.23) × 10^{12} synapses.
(9) (a) The limbic lobe is composed of the hippocampus, the parahippocampus, cingulate cortex, and the piriform cortex. The volume of hippocampus is 1.542 ± 1.12 cm^3 [Simic *et al.*, 1997]. The volume of the parahippocampus is: 4.3 ± 0.9 cm^3 (anterior) and 4.1 ± 1.2 cm^3 (posterior), for a total of 8.4 ± 2.1 cm^3 [Kennedy *et al.*, 1998]; others reported 7.1 ± 0.86 cm^3 [Raz, 2004]. The volume of the male cingulate cortex is estimated as 9.32 ± 2.39 cm^3 (left hemisphere) and 8.60 ± 2.06 cm^3 (right hemisphere) [Highley *et al.*, 2001], total volume 17.92 ± 4.45 cm^3 [Highley *et al.*, 2001]. The volume of the piriform cortex and cortical amygdala is estimated as 530 ± 59 mm^3 (right cortex) and 512 ± 60 mm^3 (left cortex) [Pereira *et al.*, 2005]. Total limbic lobe volume is thus estimated as: 27.6 cm^3.
(b) The hippocampus has five main subdivisions (granule cell layer, hilus, CA3−2, CA1, and subiculum) with the following mean numbers of neurons in each subdivision: granule cell layer 15 × 10^6 (0.28), hilus 2.0 × 10^6 (0.16), CA3-2 2.7 × 10^6 (0.22), CA1 16 × 10^6 (0.32), subiculum 4.5 × 10^6 (0.19) [West and Gundersen, 1990; Schumann and Amaral, 2005], giving a total of 4.02 × 10^7 neurons. The total number of neurons in the hippocampus was also reported as (4.85 ± 0.84) × 10^7 [Simic *et al.*, 1997]. The synaptic densities in the hippocampal subiculum and CA1 were reported as (11.98 ± 1.69) × 10^8/mm^3 (subiculum) and (14.51 ± 3.81) × 10^8/mm^3 (CA1) [Alonso-Nanclares *et al.*, 2011]. The neocortex neuron density was estimated as (50.4 ± 11.08) × 10^6/cm^3 with the numerical density in each of the four neocortex lobes as follows: frontal lobe 40.9 × 10^6/cm^3 (0.30), temporal lobe 44.6 × 10^6/cm^3 (0.20), parietal lobe 49.8 × 10^6/cm^3 (0.18), occipital lobe 93.0 × 10^6/cm^3 (0.27) [Bundgaard, 2001].
(10) The number of neurons in the cerebral cortex is estimated as 2.8 × 10^{10} [Bundgaard, 2001] and (1.634 ± 2.17) × 10^{10} [Azevedo *et al.*, 2009]. There seems to be no estimate for the number of neurons in the neocortex smaller than 1.634 × 10^{10} [Azevedo *et al.*, 2009].
(11) Others estimated 6.61 × 10^9 [Bundgaard, 2001], including 7.82 × 10^9 (0.25) (male) and 6.59 × 10^9 (0.24) (female) [Pakkenberg and Gundersen, 1997].
(12) For the whole occipital lobe, others estimated 4.67 × 10^9 [Bundgaard, 2001], including 4.89 × 10^9 (0.22) (male) and 4.28 × 10^9 (0.28) (female) [Pakkenberg and Gundersen, 1997].
(13) For the parietal lobe, others estimated 5.10 × 10^9 [Bundgaard, 2001], including 5.51 × 10^9 (0.28) (male) and 4.50 × 10^9 (0.28) (female) [Pakkenberg and Gundersen, 1997].
(14) For the temporal lobe, others estimated 4.13 × 10^9 [Bundgaard, 2001], including 4.21 × 10^9 (0.34) (male) and 3.59 × 10^9 (0.31) (female) [Pakkenberg and Gundersen, 1997].

(*Continued*)

Table 2. (*Continued*)

(15) There are approximately 12.21×10^6 neurons in the human amygdaloid complex with more than 50% residing in the lateral and basal nuclei [Schumann and Amaral, 2005]. The mean number of neurons for each region is 4.00×10^6 (lateral nucleus), 3.24×10^6 (basal nucleus), 1.28×10^6 (accessory basal nucleus), 0.36×10^6 (central nucleus) and 3.33×10^6 (remaining nuclei).
(16) Total neuron numbers are reported as 32.7×10^6 (caudate nucleus), 35.4×10^6 (Putamen), 2.43×10^6 (nucleus accumbens), 3.79×10^6 (mediodorsal nucleus of the thalamus), and 4.43×10^6 (lateral nucleus of the amygdala) [Kreczmanski, 2007]. Assuming the number of neurons is 7.875×10^6 [Kreczmanski, 2007] and assuming an average of $(6.94 \pm 1.11) \times 10^3$ synapses per neuron (as in the human cerebral cortex [Tang *et al.*, 2003]), the thalamus would have $(5.47 \pm 0.87) \times 10^{10}$ synapses.
(17) The number of neurons in the human cerebellum was estimated as 1.05×10^{11} [Andersen *et al.*, 1992] with between $1.01-1.09 \times 10^{11}$ granule cells and $28-30.5 \times 10^6$ Purkinje cells [Andersen and Pakkenberg, 2003; Andersen *et al.*, 1992], with subsequent work refining these latter estimates to 1.087×10^{11} granule cells and 28.6×10^6 Purkinje cells [Andersen *et al.*, 2003]. However, the cerebellum was most recently estimated to have $0.6903 \pm 0.0665 \times 10^{11}$ neurons [Azevedo *et al.*, 2009] which is the figure we adopt here.
(18) The anterior olfactory nucleus was reported to be poorly studied in the literature [Brunjes *et al.*, 2005].
(19) There are no published studies on synapse counts in the human cerebellum because the currently available stereological methods are not well suited for synapses and would not permit counting in a reasonable time [A. S. Karlsen, private communication, 2011]. The cerebellum (of rats) was reported to have a synaptic density between $3-4 \times 10^8/\text{mm}^3$ [Kleim, 2002] but others report a synaptic density (also for rats) of $2 \times 10^8/\text{mm}^3$ [Black *et al.*, 1990]. The average volume of the cerebellum has been reported from a low of $60.11\,\text{cm}^3$ to a high of $170.6\,\text{cm}^3$ [Kandel *et al.*, 2000; Andreasen, 1996], and as $117.75 \pm 10.7\,\text{cm}^3$ (males) and $111.83 \pm 8.0\,\text{cm}^3$ (females). The human cerebellum white matter volume was estimated as $31.9\,\text{cm}^3$ and the cortex volume as $90.8\,\text{cm}^3$ for a total of $124.8\,\text{cm}^3$ [Andersen *et al.*, 2003]. Assuming a representative synaptic density of $4 \times 10^8/\text{mm}^3$ and a cerebellum cortex volume of $90.8\,\text{cm}^3$ yields an estimate of 0.363×10^{14} synapses. The total number of human cerebellum Purkinje cells and granule cells are 28×10^6 (C.V. = 0.16) and 109×10^9 (C.V. = 0.17), respectively [Andreasen, 1996]. The number of synapses per Purkinje cell was early estimated as 8×10^5 neurons/cell [Black *et al.*, 1990] but more recently as 1.74×10^5 [Napper, 2004]. Since the number of Purkinje cells (28×10^6) is small in relation to the number of granule cells (109×10^9), the high number of synapses per Purkinje cell (1.74×10^5) has minimal impact on the total number of synapses in the cerebellum (estimated as 0.363×10^{14} synapses). Assuming the cerebellum has 109×10^9 neurons and 0.363×10^{14} synapses, then each cerebellum granule cell would have only 333 synapses per granule cell, which seems very low when compared to the average 6,940 synapses per neuron in the human cerebral cortex [Tang *et al.*, 2003]. The synapse-to-neuron ratio in rat cerebellar cortex is indeed reported have an average of 338 synapses per granule cell with a maximum of 707 synapses per granule cell [Warren and Bedi, 1989]. In rats the radical difference in the number of synapses per neuron from the frontal cortex to the cerebellum has been known for decades, with the frontal cortex having $22\,270 \pm 3250$ synapses per neuron and the cerebellum having 495 ± 25 synapses per neuron [Bedi *et al.*, 1980]. The number of neurons in the human neocortex is ∼4 times smaller than the number of neurons in the human cerebellum [Azevedo *et al.*, 2009], but since each cerebral cortex neuron has ∼16 times more synapses per neuron than each cerebellum granule cell and the number of Purkinje cells is relatively low, the cerebral cortex seems to contribute ∼four-fold more to the final estimate of the number of human brain synaptic processed bits per second. Taking the minimum synaptic density reported between $2-4 \times 10^8/\text{mm}^3$ [Black *et al.*, 1990] and the cerebellum volume of $90.8\,\text{cm}^3$ [Andersen *et al.*, 2003] we would obtain $1.82-3.63 \times 10^{13}$ synapses, but assuming $(0.6903 \pm 0.0665) \times 10^{11}$ neurons [Azevedo *et al.*, 2009] and 707 synapses per granule cell [Warren and Bedi, 1989] implies $4.41-5.35 \times 10^{13}$ synapses — so $(3.35 \pm 1.54) \times 10^{13}$ synapses seems a reasonable midrange value to adopt.

(*Continued*)

Table 2. (*Continued*)

(20) The average numbers of synapses per neuron in the cerebral cortex are estimated as 4.38×10^3 (occipital), 7.36×10^3 (parietal), 7.52×10^3 (temporal) and 7.48×10^3 (frontal) [Tang *et al.*, 2003]. The total neocortex is estimated to average 6.94×10^3 synapses per neuron [Tang *et al.*, 2003], thus for the frontal cortex the number of synapses would be 5.012×10^{13} synapses, assuming 6.7×10^9 neurons [Pedersen, 2005] and 7.48×10^3 synapses per neuron [Tang *et al.*, 2003], close to the 5.89×10^{13} figure from [Tang *et al.*, 2001, 2003].
(21) Estimate based on neocortex percentages of the different types of electrophysiological types of neurons.
(22) Assuming 6.94×10^3 synapses per neuron (as found in the human neocortex [Tang *et al.*, 2003]) the $(1.22 \pm 0.13) \times 10^7$ neurons would correspond to $(8.47 \pm 0.90) \times 10^{10}$ synapses.
(23) Others have reported the percentages as 60.5% (irregular), 24% (tonic) and 15.5% (oscillatory) [Rodriguez-Oroz *et al.*, 2001].
(24) Avoli [1994] estimated 63% of regular spiking neurons and 37% of bursting neurons. As no data was found for the percentage of fast-spiking neurons, we assumed a percentage of 3% based on the estimate of Steriade *et al.* [1998] for the neocortex percentage of fast-spiking neurons, leaving 61% for regular spiking neurons and 36% for bursting neurons.
(25) The percentage of bursting neurons was estimated as $(3 + 6 + 7)/(6 + 28 + 19) = 0.30$ [Tasker and Dudek, 1991]. The percentage of regular spiking and fast spiking neurons are based on the proportions of electrophysiological types of neurons in the neocortex.
(26) Value for the subthalamic nucleus. Assuming number of neurons 5.61×10^5 and assuming an average of 6.94×10^3 synapses per neuron (as in the human cerebral cortex [Tang *et al.*, 2003]), the subthalamus would have 3.89×10^9 synapses.
(27) The human hypothalamus volume was reported as $4\,\text{cm}^3$ [Hofman, 1997]. Assuming a neuron density of $(50.4 \pm 11.08) \times 10^6/\text{cm}^3$ (similar to the neocortex), the total number of neurons in the human hypothalamus would be $(2.02 \pm 0.47) \times 10^8$ neurons. Assuming a synaptic density of 11.05×10^8 synapses/mm^3 (± 0.41 S.E.M), the hypothalamus would have 4.42×10^{12} synapses.
(28) The human medulla oblongata volume was estimated as $5.7\,\text{cm}^3$. Assuming a neuron density of $(50.4 \pm 11.08) \times 10^6/\text{cm}^3$ (similar to the neocortex), the total number of neurons in the human midbrain is $(2.87 \pm 0.63) \times 10^8$ neurons. The medullary nuclei was estimated to have 1.3197×10^6 neurons [Porzionato *et al.*, 2008]. Assuming an average of $(6.94 \pm 1.11) \times 10^3$ synapses per neuron (as in the human cerebral cortex [Tang *et al.*, 2003]) we obtain an estimate of $(1.99 \pm 0.32) \times 10^{12}$ synapses.
(29) The average brainstem volume was estimated as $34\,\text{cm}^3$ [Ekinci *et al.*, 2008]. The brainstem includes the medulla oblongata, the pons, and the midbrain. Total brainstem volume as well as pons and medulla have no age-related decline and both genders have similar total or regional brainstem volumes, averaging $\sim 4.7\,\text{cm}^3$ (midbrain), $\sim 19.1\,\text{cm}^3$ (pons), and $\sim 5.7\,\text{cm}^3$ (medulla). Assuming a neuron density of $(50.4 \pm 11.08) \times 10^6/\text{cm}^3$ (similar to the neocortex), the total human brainstem population would be $(1.713 \pm 0.376) \times 10^9$ neurons. If we subtract the neuron counts estimated for the medulla oblongata $(2.87 \pm 0.63) \times 10^8$ and for the pons $(9.63 \pm 2.12) \times 10^8$, we obtain an estimate for the midbrain of 4.63×10^8 neurons; allocating this latter number equally into the three midbrain subregions (tectum, tegmentum, and pretectal region) gives 1.54×10^8 neurons for each. The midbrain thus has $(3.21 \pm 0.51) \times 10^{12}$ synapses assuming an average of $(6.94 \pm 1.11) \times 10^3$ synapses per neuron as in the human cerebral cortex [Tang *et al.*, 2003], also implying $(1.07 \pm 0.17) \times 10^{12}$ synapses for each of the three subregions. Taking midbrain volume to be $\sim 4.7\,\text{cm}^3$ and assuming a neuron density of $(50.4 \pm 11.08) \times 10^6/\text{cm}^3$ (similar to the neocortex), we obtain an estimate of $(2.37 \pm 0.52) \times 10^8$ neurons in the midbrain.

(*Continued*)

Table 2. (*Continued*)

(30) The average pons volume was estimated as $19.1\,\mathrm{cm}^3$ [Ekinci *et al.*, 2008]. Assuming a neuron density of $(50.4 \pm 11.08) \times 10^6/\mathrm{cm}^3$ (similar to the neocortex), the human pons has $(9.63 \pm 2.12) \times 10^8$ neurons. Taking a synaptic density of 11.05×10^8 synapses/mm^3 (± 0.41 S.E.M.), the midbrain would have 2.11×10^{13} synapses. Assuming an average of $(6.94 \pm 1.11) \times 10^3$ synapses per neuron (as in the human cerebral cortex [Tang *et al.*, 2003]) the pons has $(6.68 \pm 1.06) \times 10^{12}$ synapses.

(31) The basal ganglia has an estimated $(4.15 \pm 0.99) \times 10^8$ neurons [Karlsen and Pakkenberg, 2011]. Assuming an average of 6.94×10^3 synapses per neuron (as in the human cerebral cortex [Tang *et al.*, 2003]) the human basal ganglia has a total of $(2.88 \pm 0.69) \times 10^{12}$ synapses.

(32) The volume of the clustrum is reported as 0.025% of the cerebral cortex, thus $(517\,\mathrm{cm}^3)/400 = 1.29\,\mathrm{cm}^3$ [Crick and Koch, 2005; Kowianski *et al.*, 1999; Nieuwenhuys, 2008]. Assuming a neuron density of $(50.4 \pm 11.08) \times 10^6/\mathrm{cm}^3$ (similar to the neocortex), the total number of neurons in the cerebral nuclei claustrum would be 6.50×10^7 neurons. Taking an average of $6.94 \pm 1.11 \times 10^3$ synapses per neuron (as in the human cerebral cortex [Tang *et al.*, 2003]) for the clustrum implies a total of $(4.51 \pm 0.72) \times 10^{11}$ synapses.

(33) The human cerebral nuclei has a volume between $44.7\,\mathrm{cm}^3$ [Pakkenberg and Gundersen, 1997] and $42.8\,\mathrm{cm}^3$ (0.13) [García-Fiñana, 2003]. At a neuron density of $(50.4 \pm 11.08) \times 10^6/\mathrm{cm}^3$ (similar to the neocortex) the neuron count in the human cerebral nuclei would be $(2.25 \pm 0.50) \times 10^9$. The estimated number of neurons for the anterior olfactory nucleus and the basal forebrain together is 1.76×10^9 neurons; allocating 10% to the anterior olfactory nucleus and 90% to the basal forebrain yields 1.58×10^9 neurons for the basal forebrain and 1.76×10^8 neurons for the anterior olfactory nucleus. Assuming an average of $(6.94 \pm 1.11) \times 10^3$ synapses per neuron (as in the human cerebral cortex [Tang *et al.*, 2003]) we obtain $(1.10 \pm 0.18) \times 10^{13}$ synapses for the basal forebrain and $(1.22 \pm 0.20) \times 10^{12}$ synapses for the anterior olfactory nucleus.

sensory information — individual elements of information are represented not by the spiking activity of a single cell but rather by the activity of populations or clusters of neurons that strongly interact. Population codes can support computations such as noise removal and nonlinear mapping that might reduce total sensor burden since loss of information from a single cell may not significantly degrade the interpretation of overall spike activity.

5. Conclusions

This paper uses a novel electrophysiological approach to estimate the data rate requirements for acquiring, transmitting, and storing continuous real-time single-neuron electrical information from the human brain. We conclude that the task of monitoring raw data traffic for an entire living human brain, e.g., by employing *in vivo* neural nanorobotics systems, will require a network data handling capacity of $(5.52 \pm 1.13) \times 10^{16}$ bits/sec, corresponding to an estimated synaptic-processed spike rate of $(4.31 \pm 0.86) \times 10^{15}$ spikes/sec which is the event detection requirement for the entire embedded *in vivo* sensor system in the context of nanorobotic whole-brain monitoring. Non-electrical channels must also be recorded but the data processing requirements for these additional channels are expected to be far less demanding.

Acknowledgments

The principal author (NRBM) thanks the Fundação para a Ciência e Tecnologia (FCT) for their financial support of this work (grant SFRH/BD/69660/2010).

Appendix A

Abbreviations

RS — Regular Spiking
FS — Fast Spiking
B — Bursting
SWS — Slow Wave Sleep
REM sleep — Rapid Eye Movement Sleep
LTP — Long-Term Potentiation
LTD — Long-Term Depression
ALS — Amyotrophic Lateral Sclerosis

References

Adelman, L. T., Bialek, W. and Olberg, R. M. [2003] "The information content of receptive fields," *Neuron* **40**, 823−833.

Allers, K. A. and Sharp, T. [2003] "Neurochemical and anatomical identification of fast- and slow-firing neurones in the rat dorsal raphe nucleus using juxtacellular labelling methods *in vivo*," *Neuroscience* **122**, 193−204.

Allman, J. M. [2010] "The von Economo neurons in frontoinsular and anterior cingulate cortex in great apes and humans," *Brain Structure and Function* **214**(5−6), 495−517.

Alonso-Nanclares, L., Kastanauskaite, A., Rodriguez, J., Gonzalez-Soriano, J. and DeFelipe, J. [2011] "A stereological study of synapse number in the epileptic human hippocampus," *Frontiers in Neuroanatomy* **5**, 8.

Andersen, B. B., Korbo, L. and Pakkenberg, B. [1992] "A quantitative study of the human cerebellum with unbiased stereological techniques," *Journal of Comparative Neurology* **326**, 549−560.

Andersen, B. B., Gundersen, H. J. and Pakkenberg, B. [2003] "Aging of the human cerebellum: A stereological study," *Journal of Comparative Neurology* **466**, 356−365.

Andersen, B. B. and Pakkenberg, B. [2003] "Stereological quantitation in cerebella from people with schizophrenia," *The British Journal of Psychiatry* **182**, 354−361, doi: 10.1192/bjp.02.65.

Anderson, J. R., Jones, B. W., Watt, C. B., Shaw, M. V., Yang, J. H., Demill, D., Lauritzen, J. S., Lin, Y., Rapp, K. D., Mastronarde, D., Koshevoy, P., Grimm, B., Tasdizen, T., Whitaker, R. and Marc, R. E. [2011] "Exploring the retinal connectome," *Molecular Vision* **17**, 355−379.

Andreasen, N. C. [1996] "Automatic atlas-based volume estimation of human brain regions from MR images," *Journal of Computer Assisted Tomography* **20**(1), 98−106.

Astier, Y., Bayley, H. and Howorka, S. [2005] "Protein components for nanodevices," *Current Opinion in Chemical Biology* **9**(6), 576−584.

Avoli, M. [1994] "Electrophysiological and repetitive firing properties of neurons in the superficial/middle layers of the human neocortex maintained *in vitro*," *Experimental Brain Research* **98**(1), 135−144.

Azevedo, F. A., Carvalho, L. R., Grinberg, L. T., Farfel, J. M., Ferretti, R. E., Leite, R. E., Jacob Filho, W., Lent, R. and Herculano-Houzel, S. [2009] "Equal numbers of neuronal and nonneuronal cells make the human brain an isometrically scaled-up primate brain," *Journal of Comparative Neurology* **513**(5), 532−541.

Barry, W. C. and Gutnickb, M. J. [1990] "Intrinsic firing patterns of diverse neocortical neurons," *Trends in Neuroscience* **13**(3), 99−104.

Bean, B. P. [2007] "The action potential in mammalian central neurons," *Nature Reviews Neuroscience* **8**, 451−465.

Bedi, K. S., Thomas, Y. M., Davies, C. A. and Dobbing, J. [1980] "Synapse-to-neuron ratios of the frontal and cerebellar cortex of 30-day-old and adult rats undernourished during early postnatal life," *The Journal of Comparative Neurology* **193**(1), 49−56.

Beurrier, C., Congar, P., Bioulac, B. and Hammond, C. [1999] "Subthalamic nucleus neurons switch from single-spike activity to burst-firing mode," *The Journal of Neuroscience* **19**(2), 599−609.

Bialek, W. [1993] "Bits and brains: Information flow in the nervous system," *Physica A: Statistical Mechanics and Its Applications* **200**(1−4), 581−593.

Bialek, W. and Rieke, F. [1992] "Reliability and information transmission in spiking neurons," *Trends in Neuroscience* **15**(11), 428−434.

Black, J. E., Isaacs, K. R., Anderson, B. J., Alcantara, A. A. and Greenough, W. T. [1990] "Learning causes synaptogenesis, whereas motor activity causes angiogenesis, in cerebellar cortex of adult rats," *Proceedings of National Academy of Science USA* **87**, 5568−5572.

Bliss, T. V. P. and Collingridge, G. L. [1993] "A synaptic model of memory: Long-term potentiation in the hippocampus," *Nature* **361**, 31−39.

Borst, A. and Theunissen, F. E. [1999] "Information theory and neural coding," *Nature Neuroscience* **2**(11).

Bostrom, N. [1998] "How long before superintelligence?" *International Journal of Future Studies* **2**.

Braendgaard, H., Evans, S. M., Howard, C. V. and Gundersen, H. J. [1990] "Total number of neurons in the human neocortex unbiasedly estimated using optical disectors," *Journal of Microscopy* **157**, 285–304.

Brenner, N. [2000] "Synergy in a neural code," *Neural Computation* **12**, 1531–1552.

Brunjes, P. C., Illig, K. R. and Meyer, E. A. [2005] "A field guide to the anterior olfactory nucleus (cortex)," *Brain Research Reviews* **50**(2), 305–335.

Bundgaard, M. J. [2001] "Size of neocortical neurons in control subjects and in Alzheimer's disease," *Journal of Anatomy* **198**, 481–489.

Buracas, G. T. and Albright, T. D. [1999] "Gauging sensory representations in the brain," *Trends in Neuroscience* **22**(7), 303–309.

Cauli, B., Audinat, E., Lambolez, B., Angulo, M. C., Ropert, N., Tsuzuki, K., Hestrin, S. and Rossier, J. [1997] "Molecular and physiological diversity of cortical nonpyramidal cells," *Journal of Neuroscience* **17**, 3894–3906.

Cavalcanti, A. and Freitas, R. A., Jr. [2003] "Nanosystem design with dynamic collision detection for autonomous nanorobot motion control using neural networks," *Computer Graphics and Geometry* **5**, 50–74, `http://www.cgg-journal.com/2003-1/03.htm`.

Cavalcanti, A., Shirinzadeh, B., Freitas, R. A., Jr. and Hogg, T. [2008] "Nanorobot architecture for medical target identification," *Nanotechnology* **19**, 015103, `http://www.iop.org/EJ/article/0957-4484/19/1/015103/nano8_1_015103.pdf`.

Chang, Y.-M. and Luebke, J. I. [2007] "Electrophysiological diversity of layer 5 pyramidal cells in the prefrontal cortex of the Rhesus monkey: *In vitro* slice studies," *Journal of Neurophysiology* **98**(5), 2622–2632.

Colbert, C. M. and Johnston, D. [1996] "Axonal action-potential initiation and Na^+ channel densities in the soma and axon initial segment of subicular pyramidal neurons," *Journal of Neuroscience* **16**, 6676–6686.

Connors, B. W., Gutnick, M. J. and Prince, D. A. [1982] "Electrophysiological properties of neocortical neurons *in vitro*," *Journal of Neurophysiology* **48**, 1302–1320.

Crick, F. C. and Koch, C. [2005] "What is the function of the claustrum?" *Philosophical Transaction of the Royal Society B: Biological Science* **360**, 1271–1279, doi: 10.1098/rstb.2005.166.

Crotty, P., Sangrey, T. and Levy, W. B. [2006] "Metabolic energy cost of action potential velocity," *Journal of Neurophysiology* **96**, 1237–1246.

DeFelipe, J. [1999] "Estimation of the number of synapses in the cerebral cortex: Methodological considerations," *Cerebral Cortex* **9**(7), 722–732, doi: 10.1093/cercor/9.7.722.

Diego, C. [2004] "Electrophysiological classes of neocortical neurons," *Neural Networks* **17**(5–6), 633–646.

Dix, A. [2007] "The brain and the web: A quick backup in case of accidents," *Interfaces* **65**, 6–7.

Duijnhouwer, J., Remme, M. W. H., van Ooyen, A. and van Pelt, J. [2001] "Influence of dendritic topology on firing patterns in model neurons," *Neurocomputing* **38–40**; 183–189.

Eccles, J. [1957] *The Physiology of Nerve Cells* (Baltimore).

Ekinci, N., Acer, N., Akkaya, A., Sankur, S., Kabadayi, T. and Sahin, B. [2008] "Volumetric evaluation of the relations among the cerebrum, cerebellum and brain stem in young subjects: A combination of stereology and magnetic resonance imaging," *Surgical and Radiologic Anatomy* **30**(6), 489–494.

Faber, E. S. L., Callister, R. J. and Sah, P. [2001] "Morphological and electrophysiological properties of principal neurons in the rat lateral amygdala *in vitro*," *Journal of Neurophysiology* **85**, 714–723.

Faulkner, B. and Brown, T. H. [1999] "Morphology and physiology of neurons in the rat perirhinal-lateral amygdala area," *Journal of Comparative Neurology* **411**, 613–642.

Fiala, J. C. [2007] Synapses.Bu.Edu, http://synapses.clm.utexas.edu/index.asp.

Fischer, C. P. [1999] "Preferential loss of large neocortical neurons during HIV infection: A study of the size distribution of neocortical neurons in the human brain," *Brain Research* **828**(1−2), 119−126.

Foehring, R. C. [1990] "Two patterns of firing in human neocortical neurons," *Neuroscience Letters* **110**(3), 279−285.

Franceschetti, S., Guatteo, E., Panzica, F., Sancini, G., Wanke, E. and Avanzini, G. [1995] "Ionic mechanisms underlying burst firing in pyramidal neurons: Intracellular study in rat sensorimotor cortex," *Brain Research* **696**, 127−139.

Freitas, R. A., Jr. [1998] "Exploratory design in medical nanotechnology: A mechanical artificial red cell," *Artificial Cells, Blood, Substitutes, and Immobilization, Biotechnology* **26**, 411−430, http://www.foresight.org/Nanomedicine/Respirocytes.html.

Freitas, R. A., Jr. [1999a] *Nanomedicine, Volume I: Basic Capabilities* (Landes Bioscience, Georgetown, TX), http:www.nanomedicine.com/NMI.htm.

Freitas, R. A., Jr. [1999b] *Electric Field, Neurosensing, in Nanomedicine, Volume I: Basic Capabilities*, Chap. 4.8.6.1 (Landes Bioscience, Georgetown, TX, 1999), http://www.nanomedicine.com/NMI/4.8.6.1.htm.

Freitas, R. A., Jr. [2000] "Nanodentistry," *Journal of American Dental Association* **131**, 1559−1566, http://jada.ada.org/cgi/content/full/131/11/1559#SEC2.

Freitas, R. A., Jr. [2003] *Nanomedicine, Volume IIA: Biocompatibility* (Landes Bioscience, Georgetown, TX), http://www.nanomedicine.com/NMIIA.htm.

Freitas, R. A., Jr. [2005a] "What is nanomedicine?" *Nanomedicine: Nanotechnology, Biology and Medicine*, http://www.nanomedicine.com/Papers/WhatIsNMMar05.pdf.

Freitas, R. A., Jr. [2005b] "Current status of nanomedicine and medical nanorobotics (invited survey)," *Journal of Computational and Theoretical Nanoscience* **2**, 1−25. http://www.nanomedicine.com/Papers/NMRevMar05.pdf.

Freitas, R. A., Jr. [2005c] "Microbivores: Artificial mechanical phagocytes using digest and discharge protocol," *Journal of Evolution and Technology* **14**, 1−52, orig.Zyvex preprint, March 2001, http://www.jetpress.org/volume14/freitas.html.

Freitas, R. A., Jr. [2006a] "Pharmacytes: An ideal vehicle for targeted drug delivery," *Journal of Nanoscience and Nanotechnology* **6**, 2769−2775, http://www.nanomedicine.com/Papers/JNNPharm06.pdf.

Freitas, R. A., Jr. [2006b] "Progress in nanomedicine and medical nanorobotics," in *Handbook of Theoretical and Computational Nanotechnology, Volume 6, Bioinformatics, Nanomedicine, and Drug Design*, Chap. 13, eds. Rieth, M. and Schommers, W. (American Scientific Publishers, Stevenson Ranch, CA), pp. 619−672, http://www.nanomedicine.com/Papers/ProgressNM06.pdf.

Freitas, R. A., Jr. [2007] "The ideal gene delivery vector: Chromallocytes, cell repair nanorobots for chromosome replacement therapy," *Journal of Evolution and Technology* **16**, 1−97, http://jetpress.org/v16/freitas.pdf.

Freitas, R. A., Jr. [2009] "Computational tasks in medical nanorobotics," in *Bio-inspired and Nano-Scale Integrated Computing*, Chap. 15, ed. Eshaghian-Wilner, M. M. (John Wiley and Sons, NY), pp. 391−428, http://www.nanomedicine.com/Papers/NanorobotControl2009.pdf.

Freitas, R. A., Jr. [2010] "Comprehensive nanorobotic control of human morbidity and aging, in *The Future of Aging: Pathways to Human Life Extension*, Chap. 23, eds. Fahy *et al.* (Springer, New York), pp. 685−805, http://www.nanomedicine.com/Papers/Aging.pdf.

Freitas, R. A., Jr. and Phoenix, C. J. [2002] "Vasculoid: A personal nanomedical appliance to replace human blood," *Journal of Evolution and Technology* **11**, 1−139, http://www.jetpress.org/volume11/vasculoid.pdf.

Freitas, R. A., Jr. and Merkle, R. C. [2004] *Kinematic Self-Replicating Machines* (Landes Bioscience, Georgetown, TX, 2004), http://www.molecularassembler.com/KSRM.htm.

Freitas, R. A., Jr. and Merkle, R. C. [2006] "Nanofactory collaboration," http://www.molecularassembler.com/Nanofactory/.

Fuhrmann, G., Segev, I., Markram, H. and Tsodyks, M. [2002] "Coding of temporal information by activity-dependent synapses," *Journal of Neurophysiology* **87**(1), 140–148.

García-Fiñana, M. [2003] "Comparison of MR imaging against physical sectioning to estimate the volume of human cerebral compartments," *NeuroImage* **18**(2).

Haas, H. L. [2008] "Histamine in the nervous system," *Physiological Reviews* **88**, 1183–1241.

Hamam, B. N., Kennedy, T. E., Alonso, A. and Amaral, D. G. [2000] "Morphological and electrophysiological characteristics of layer V neurons of the rat medial entorhinal cortex," *Journal of Comparative Neurology* **418**, 457–472.

Hamam, B. N., Amaral, D. G. and Alonso, A. A. [2002] "Morphological and electrophysiological characteristics of layer V neurons of the rat lateral entorhinal cortex," *Journal of Comparative Neurology* **451**, 45–61.

Hameroff, S. R. [1987] *Ultimate Computing: Biomolecular Consciousness and Nanotechnology* (Elsevier Science Publishers).

Hestrin, S. and Armstrong, W. E. [1996] "Morphology and physiology of cortical neurons in layer I," *Journal of Neuroscience* **16**, 5290–5300.

Highley, J. R., Walker, M. A., Esiri, M. M., McDonald, B., Harrison, P. J. and Crow, T. J. [2001] "Schizophrenia and the frontal lober: Post-mortem stereological study of tissue volume," *British Journal of Psychiatry* **178**, 337–343.

Hofman, M. A. [1997] "Lifespan changes in the human hypothalamus," *Experimental Gerontology* **32**(4/5), 559–575.

Holtmaat, A. and Svoboda, K. [2009] "Experience-dependent structural synaptic plasticity in the mammalian brain," *Nature Reviews Neuroscience* **10**(9), 647–658.

Huttenlocher, P. R. [1979] "Synaptic density in human frontal cortex — Developmental changes and effects of aging," *Brain Research* **163**(2), 195–205.

IBM Seeks to Build the Computer of the Future Based on Insights from the Brain [2008] IBM Awarded DARPA Funding for Cognitive Computing Collaboration, http://www-03.ibm.com/press/us/en/pressrelease/26123.wss.

Izhikevich, E. M. [2004] "Which model to use for cortical spiking neurons?" *IEEE Transactions on Neural Networks* **15**, 1063–1070.

Juusola, M. [1996] "Information processing by graded-potential transmission through tonically active synapses," *Trends in Neuroscience* **19**(7), 292–297.

Kandel, E. R., Schwartz, J. H. and Jessell, T. M. [2000] *Principles of Neural Science*, 4th edition (New York, McGraw Hill).

Kandel, E. R. [2001] "The molecular biology of memory storage: A dialogue between gene and synapses," *Science* **294**(5544), 1030–1038.

Karlsen, A. S. and Pakkenberg, B. [2011] "Total numbers of neurons and glial cells in cortex and basal ganglia of aged brains with down syndrome — A stereological study," *Cerebral Cortex*.

Kennedy, D. N., Lange, N., Makris, N., Bates, J., Meyer, J. and Caviness, V. S., Jr. [1998] "Gyri of the human neocortex: An MRI-based analysis of volume and variance," *Cerebral Cortex* **8**(4), 372–384.

Kennedy, D. P. [2007] "No reduction of spindle neuron number in frontoinsular cortex in autism," *Brain and Cognition* **64**, 124–129.

Kleim, J. A. [2002] "Synapse formation is associated with memory storage in the cerebellum," *Proceedings of the National Academy of Science* **99**(2).

Kleinfeld, D., Bharioke, A., Blinder, P., Bock, D. D., Briggman, K. L., Chklovskii, D. B., Denk, W., Helmstaedter, M., Kaufhold, J. P., Lee, W. C., Meyer, H. S., Micheva, K. D., Oberlaender, M., Prohaska, S., Reid, R. C., Smith, S. J., Takemura, S., Tsai, P. S. and Sakmann, B. [2011] "Large-scale automated histology in the pursuit of connectomes," *Journal of Neuroscience* **31**(45), 16,125–16,138.

Koch, C. [1983] "Nonlinear interactions in a dendritic tree: Localization, timing, and role in information processing," *Proceedings of National Academic of Science USA* **80**(9), 2799–2802.

Koch, C. [1997] *Biophysics of Computation: Information Processing in Single Neurons* (Oxford University Press, New York).

Koch, C. and Segev, I. [2000] "The role of single neurons in information processing," *Nature Neuroscience* **3**, 1171–1177.

Kole, M. H. P., Letzkus, J. J. and Stuart, G. J. [2007] "Axon initial segment Kv1 channels control axonal action potential waveform and synaptic efficacy," *Neuron* **55**(4), 633–647.

Kostarelos, K. [2010] "Nanorobots for medicine: How close are we?" *Nanomedicine* **5**(3), 341–342.

Kowianski, P., Dziewiatkowski, J., Kowianska, J. and Morys, J. [1999] "Comparative anatomy of the claustrum in selected species: A morphometric analysis," *Brain, Behavior and Evolution* **53**, 44–54.

Kreczmanski, P. [2007] "Volume, neuron density and total neuron number in five subcortical regions in schizophrenia," *Brain* **130**(3), 678–692, doi: 10.1093/brain/awl386.

Kurzweil, R. [1999] *The Age of Spiritual Machines* (Viking, New York), p. 77.

Kuwana, S., Tsunekawa, N., Yanagawa, Y., Okada, Y., Kuribayashi, J. and Obata, K. [2006] "Electrophysiological and morphological characteristics of GABAergic respiratory neurons in the mouse pre-Botzinger complex," *European Journal of Neuroscience* **23**, 667–674.

Kuzum, D., Jeyasingh, R. G., Lee, B. and Wong, H. S. [2011] "Nanoelectronic programmable synapses based on phase change materials for brain-inspired computing," *American Chemical Society, Nano Letters*.

Lee, S. H., Govindaiah, G. and Cox, C. L. [2007] "Heterogeneity of firing properties among rat thalamic reticular nucleus neurons," *Journal of Physiology* **582**, 195–208.

Lee, S. H., Choi, J. H., Lee, N., Lee, H. R., Kim, J. I., Yu, N. K., Choi, S. L., Lee, S. H., Kim, H. and Kaang, B. K. [2008] "Synaptic protein degradation underlies destabilization of retrieved fear memory," *Science* **319**(5867), 1253–1256, Epub 2008 Feb 7.

Likhtik, E., Pelletier, J. G., Popescu, A. T. and Paré, D. [2006] "Identification of basolateral amygdala projection cells and interneurons using extracellular recordings," *Journal of Neurophysiology* **96**(6), 3257–3265.

Lionel, G. N., Azouz, R., Sanchez-Vives, M. V., Gray, C. M. and McCormick, D. A. [2003] "Electrophysiological classes of cat primary visual cortical neurons *in vivo* as revealed by quantitative analyses," *Journal of Neurophysiology* **89**(3), 1541–1566.

Llinas, R. and Ribary, U. [1993] "Coherent 40-Hz oscillation characterizes dream state in humans," *Proceedings of National Academic Science of USA* **90**(5), 2078–2081.

London, M. and Hausser, M. [2005] "Dendritic computation," *Annual Review of Neuroscience* **28**, 503–532.

Lu, J., Tapia, J. C., White, O. L. and Lichtman, J. W. [2009] "The interscutularis muscle connectome," *PLoS Biology* **7**(2), e32.

Maas, W. [1999] "Dynamic stochastic synapses as computational units," *Neural Computation* **11**(4), 903–917, `http://zadorlab.cshl.edu/PDF/Maass-Zador99.pdf`.

Malickas, A. [1996] Gradual uploading as a cognition of mind, `http://www.aleph.se/Trans/Global/Uploading/gupload.html`.

Mallouk, T. E. and Sen, A. [2009] "Powering nanorobots," *Scientific American* **300**(5), 72–77.

Manwani, A. [2001] "Detecting and estimating signals over noisy and unreliable synapses: Information-theoretic analysis," *Neural Computation* **13**(1), 1–33.

Marcus, D. S., Harwell, J., Olsen, T., Hodge, M., Glasser, M. F., Prior, F., Jenkinson, M., Laumann, T., Curtiss, S. W. and Van Essen, D. C. [2011] "Informatics and data mining tools and strategies for the human connectome project," *Frontiers in Neuroinformatics* **5**(4).

Markram, H. [1998] "Interneurons of the neocortical inhibitory system," *Journal of Neurophysiology* **79**(1), 483–490.

Martel, S., Mohammadi, M., Felfoul, O., Lu, Z. and Pouponneau, P. [2009] "Flagellated magnetotactic bacteria as controlled MRI-trackable propulsion and steering systems for medical nanorobots operating in the human microvasculature," *International Journal of Robotics Research* **28**(4), 571–582.

Mavroides, D. and Ferreira, A. (eds.) [2011] *NanoRobotics: Current Approaches and Techniques* (Springer, New York, 2011).

McGann, J. P., Moyer, J. R., Jr. and Brown, T. H. [2001] "Predominance of late-spiking neurons in layer VI of rat perirhinal cortex," *Journal of Neuroscience* **21**, 4969–4976.

Merkle, R. [1989] "Energy limits to the computational power of the human brain," *Foresight Update* **6**.

Moravec, H. [1998] "When will computer hardware match the human brain?" *Journal of Evolution and Technology* **1**.

Morris, K. [2001] "Macrodoctor, come meet the nanodoctors," *Lancet* **357**(9258), 778.

Nambu, A. and Llinas, R. [1997] "Morphology of globus pallidus neurons: Its correlation with electrophysiology in guinea pig brain slices," *Journal of Comparative Neurology* **377**, 85–94.

Napper, R. M. A. [2004] "Number of parallel fiber synapses on an individual Purkinje cell in the cerebellum of the rat," *The Journal of Comparative Neurology* **274**(2), 168–177.

Nieuwenhuys, R. [2008] *The Human Central Nervous System* (Springer, 2008).

Nishida, S., Narumoto, J., Sakai, Y., Matsuoka, T., Nakamae, T., Yamada, K., Nishimura, T. and Fukui, K. [2011] "Anterior insular volume is larger in patients with obsessive–compulsive disorder," *Progress in Neuro-Psychopharmacology and Biological Psychiatry* **35**(4), 997–1001.

Ogawa, Y. and Rasband, M. N. [2008] "The functional organization and assembly of the axon initial segment," *Current Opinion in Neurobiology* **18**(3), 307–313.

Pakkenberg, B. [1993] "Total nerve cell number in neocortex in chronic schizophrenics and controls estimated using optical disectors," *Biological Psychiatry* **34**(11), 768–772.

Pakkenberg, B. [2003] "Aging and the human neocortex," *Experimental Gerontology* **38**(1/2), 95–99.

Pakkenberg, B. and Gundersen, H. J. [1997] "Neocortical neuron number in humans: Effect of sex and age," *Journal of Comparative Neurology* **384**, 312–320.

Palay, S. L., Sotelo, C., Peters, A. and Orkand, P. M. [1968] "The axon hillock and the initial segment," *The Journal of Cell Biology* **38**, 193–201.

Palmer, L. M. and Stuart, G. J. [2006] "Site of action potential initiation in layer 5 pyramidal neurons," *The Journal of Neuroscience* **26**(6), 1854–1863.

Pang, K., Tepper, J. M. and Zaborszky, L. [1998] "Morphological and electrophysiological characteristics of noncholinergic basal forebrain neurons," *The Journal of Comparative Neurology* **394**, 186–204.

Park, H. H., Jamison, A. C. and Lee, T. R. [2007] "Rise of the nanomachine: The evolution of a revolution in medicine," *Nanomedicine* **2**(4), 425–439.

Patel, G. M., Patel, G. C., Patel, R. B., Patel, J. K. and Patel, M. [2006] "Nanorobot: A versatile tool in nanomedicine," *Journal of Drug Targeting* **14**(2), 63–67.

Pedersen, K. M. [2005] "No global loss of neocortical neurons in Parkinson's disease: A quantitative stereological study," *Movement Disorders* **20**(2), 164−171.

Pelvig, D. P., Pakkenberg, H., Regeur, L., Oster, S. and Pakkenberg, B. [2003] "Neocortical glial cell numbers in Alzheimer's disease; a stereological study," *Dementia and Geriatric Cognitive Disorders* **16**, 212−219, doi: 10.1159/000072805.

Penrose, R. [1989] *The Emperor's New Mind* (Oxford University Press, New York).

Pereira, P. M. G., Insaustid, R., Artacho-Pérulad, E., Salmenperäe, T., Kälviäinene, R. and Pitkänenf, A. [2005] "MR volumetric analysis of the piriform cortex and cortical amygdala in drug-refractory temporal lobe epilepsy," *American Journal of Neuroradiology* **26**, 319−332.

Plenz, D. and Kitai, S. T. [1998] "Up and down states in striatal medium spiny neurons simultaneously recorded with spontaneous activity in fast-spiking interneurons studied in cortex−striatum−substantia nigra organotypic cultures," *The Journal of Neuroscience* **18**(1), 266−283.

Polavieja, G. G., Harsch, A., Kleppe, I., Robinson, H. P C. and Juusola, M. [2005] "Stimulus history reliably shapes action potential waveforms of cortical neurons," *The Journal of Neuroscience* **25**(23), 5657−5665.

Popov, A. M., Lozovik, Y. E., Fiorito, S. and Yahia, L. [2007] "Biocompatibility and applications of carbon nanotubes in medical nanorobots," *International Journal of Nanomedicine* **2**(3), 361−372.

Porzionato, A., Macchi, V., Guidolin, D., Sarasin, G., Parenti, A. and De Caro, R. [2008] "Anatomic distribution of apoptosis in medulla oblongata of infants and adults," *Journal of Anatomy* **212**(2), 106−113.

Puro, D. G., De Mello, F. G. and Nirenberg, M. [1997] "Synapse turnover: The formation and termination of transient synapses," *Proceedings of National Academy Science of USA* **74**(11), 4977−4981, http://www.pnas.org/content/74/11/4977.abstract.

Raz, A., Vaadia, E. and Bergman, H. [2000] "Firing patterns and correlations of spontaneous discharge of pallidal neurons in the normal and the tremulous 1-methyl-4-phenyl-1,2,3,6-tetrahydropyridine vervet model of parkinsonism," *Journal of Neuroscience* **20**(22), 8559−8571.

Raz, N. [2004] "Aging, sexual dimorphism, and hemispheric asymmetry of the cerebral cortex: Replicability of regional differences in volume," *Neurobiology of Aging* **25**(3), 377−396.

Rieke, F., Warland, D., deRuyter and Bialek, W. [1997] *Spikes: Exploring the Neural Code* (Cambridge, MA: MIT Press).

Rodriguez-Oroz, M. C., Rodriguez, M., Guridi, J. K., Mewes, K., Chockkman, V., Vitek, J., Delong, M. R. and Obeso, J. A. [2001] "The subthalamic nucleus in Parkinson's disease: Somatotopic organization and physiological characteristics," *Brain* **124**(9), 1777−1790, doi: 10.1093/brain/124.9.1777.

Rollenhagen, A. and Lübke, J. H. R. [2006] "The morphology of excitatory central synapses: From structure to function," *Cell and Tissue Research* **326**, 221−237, http://www.springerlink.com/content/dl70582541203r82/fulltext.pdf.

Rollenhagen, A., Satzler, K., Rodriguez, E. P., Jonas, P., Frotscher, M. and Lubke, J. H. R. [2007] "Structural determinants of transmission at large hippocampal mossy fiber synapses," *Journal of Neuroscience* **27**(39), 10,434−10,444.

Sandberg, A. and Bostrom, N. [2008] "Whole brain emulation: A roadmap, technical report #2008.3," *Future of Humanity Inst., Oxford University*, www.fhi.ox.ac.uk/reports/2008-3.pdf.

Sarpeshka, R. [1997] "Efficient precise computation with noisy components: Extrapolating from an electronic cochlea to the brain," *California Institute of Technology, Pasadena, California 1997*, PhD Thesis, http://www.rle.mit.edu/avbs/documents/thesis.pdf.

Sarpeshka, R. [1998] "Analog versus digital: Extrapolating from electronics to neurobiology," *Neural Computation* **10**(7), http://www.rle.mit.edu/avbs/publications/journal_papers/analog_vs_digital.pdf.

Schumann, C. M. and Amaral, D. G. [2005] "Stereological estimation of the number of neurons in the human amygdaloid complex," *Journal of Comparative Neurology* **491**(4), 320−329.

Scorcioni, R., Lazarewicz, M. T. and Ascoli, G. A. [2004] "Quantitative morphometry of hippocampal pyramidal cells: Differences between anatomical classes and reconstructing laboratories," *Ascolithe Journal of Comparative Neurology* **473**, 177−193.

Seitz, B. T. [2007] "The great gray ravelled knot," http://hiqnews.megafoundation.org/The_Great_Gray_Ravelled_Knot.htm.

Seun, H. S. [2011] "Neuroscience: Towards functional connectomics," *Nature* **471**, 170−172.

Simic, G., Kostovic, I., Winblad, B. and Bogdanovic, N. [1997] "Volume and number of neurons of the human hippocampal formation in normal aging and Alzheimer's disease," *Journal of Comparative Neurology* **379**(4), 482−494.

Sporns, O., Tononi, G. and Kötter, R. [2005] "The human connectome: A structural description of the human brain," *PLoS Computational Biology* **1**(4), e42, doi: 10.1371/journal.pcbi.0010042.

Staiger, J. F., Flagmeyer, I., Schubert, D., Zilles, K., Kotter, R. and Luhmann, H. J. [2004] "Functional diversity of layer IV spiny neurons in rat somatosensory cortex: Quantitative morphology of electrophysiologically characterized and biocytin labeled cells," *Cerebral Cortex* **14**, 690−701.

Steriade, M. [2004] "Neocortical cell classes are flexible entities," *Nature Reviews Neuroscience* **5**(2), 121.

Steriade, M., Timofeev, I., Durmuller, N. and Grenier, F. [1998] "Dynamic properties of corticothalamic neurons and local cortical interneurons generating fast rhythmic (30−40 Hz) spike burst," *Journal of Neurophysiology* **79**(1), 483−490.

Steriade, M., Timofeev, I. and Grenier, F. [2001] "Natural waking and sleep states: A view from inside neocortical neurons," *Journal of Neurophysiology* **85**(5), 1969−1985.

Strong, S. P., Koberle, R., van Steveninck, R. R. de R. and Bialek, W. [1998] "Entropy and information in neural spike trains," *Physical Review Letters* **80**(1), 197−200.

Stuart, G. J. and Sakmann, B. [1994] "Active propagation of somatic action potentials into neocortical pyramidal cell dendrites," *Nature* **367**, 69−72.

Takakusaki, K., Shiroyama, T. and Kitai, S. T. [1997] "Two types of cholinergic neurons in the rat tegmental pedunculopontine nucleus: Electrophysiological and morphological characterization," *Neuroscience* **79**, 1089−1109.

Tang, Y., Nyengaard, J. R., De Groot, D. M. and Gundersen, H. J. [2001] "Total regional and global number of synapses in the human brain neocortex," *Synapse* **41**(3), 258−273.

Tang, Y., Nyengaard, J. R., Pakkenberg, B. and Gundersen, H. J. [2003] "Stereology of neuronal connections (myelinated fibers of white matter and synapses of neocortex) in human brain," *Image Analysis and Stereology* **22**, 171−182.

Tasker, J. G. and Dudek, F. E. [1991] "Electrophysiological properties of neurones in the region of the paraventricular nucleus in slices of rat hypothalamus," *Journal of Physiology* **434**, 271−293.

Tavares, A. [2006] "Padrões De Descarga Neuronal Na Região De CA1 Do Hipocampo De Pacientes Com Epilepsia Do Lobo Temporal E De Ratos Com Epilepsia Induzida Pela Pilocarpina: Um Estudo Comparativo, Universidade Federal do Rio Grande do Sul," http://www.lume.ufrgs.br/bitstream/handle/10183/11246/000610518.pdf.

Thagard, P. [2002] "How molecules matter to mental computation," *Philosophy of Science* **69**, 429–446.

Türe, U., Yaşargil, D. C., Al-Mefty, O. and Yaşargil, M. G. [1999] "Topographic anatomy of the insular region," *Journal of Neurosurgery* **90**(4), 720–733.

Tuszynski, J. [2006] "The dynamics of c-termini of microtubules in dendrites: A possible clue for the role of neural cytoskeleton in the functioning of the brain," *Journal of Geoethical Nanotechnology*, `http://www.aleph.se/Trans/Individual/Cryonics/neurosusp_upload.txt`.

von Neumann, J. [1958] *The Computer and the Brain* (Yale University Press).

Wang, X. J. [1999] "Fast burst firing and short-term synaptic plasticity: A model of neocortical chattering neurons," *Neuroscience* **89**(2), 347–362.

Wang, Z. and McCormick, D. A. [1993] "Control of firing mode of corticotectal and corticopontine layer V burst-generating neurons by norepinephrine, acetylcholine, and 1S,3R-ACPD," *Journal of Neuroscience* **13**(5), 2199–2216.

Warren, M. A. and Bedi, K. S. [1989] "Synapse-to-neuron ratios in rat cerebellar cortex following lengthy periods of undernutrition," *Journal of Anatomy* **170**, 173–182.

Weiss, T. and Veh, R. W. [2011] "Morphological and electrophysiological characteristics of neurons within identified subnuclei of the lateral habenula in rat brain slices," *Neuroscience* **172**, 74–93.

West, M. J. and Gundersen, H. J. G. [1990] "Unbiased stereological estimation of the number of neurons in the human hippocampus," *The Journal of Comparative Neurology* **296**(1), 1–22.

Wilson, C. J. [1981] "Spontaneous firing patterns of identified spiny neurons in the rat neostriatum," *Brain Research* **220**(1), 67–80.

Wilson, F. A., O'Scalaidhe, S. P. and Goldman-Rakic, P. C. [1994] "Functional synergism between putative y-aminobutyrate-containing neurons and pyramidal neurons in prefrontal cortex," *Proceedings Natural Academic of Science of USA* **91**(9), 4009–4013.

Wilson, H. R. [1999] "Simplifed dynamics of human and mammalian neocortical neurons," *Journal of Theoretical Biology* **200**(4), 375–388.

Wu, S. H. and Kelly, J. B. [1995] "*In vitro* brain slice studies of the rat's dorsal nucleus of the lateral lemniscus: II. Physiological properties of biocytin-labeled neurons," *Journal of Neurophysiology* **73**, 794–809.

Xu, H., Pan, F., Yang, G. and Gan, W. [2007] "Choice of cranial window type for *in vivo* imaging affects dendritic spine turnover in the cortex," *Nature Neuroscience* **10**, 549–551.

Zachary, F. [1996] "Influence of dendritic structure on firing pattern in model neocortical neurons," *Nature* **382**, 363–366.

Zador, A. [1998] "Impact of synaptic unreliability on the information transmitted by spiking neurons," *Journal of Neurophysiology* **79**(3), 1219–1229.

Zhang, X. [2008] "A mathematical model of a neuron with synapses based on physiology," *Nature Proceedings*, `http://precedings.nature.com/documents/1703/version/1/files/npre20081703-1.pdf`.